Novel Spirosuccinimide Aldose Reductase Inhibitors Derived from Isoquinoline-1,3-diones: 2-[(4-Bromo-2-fluorophenyl)methyl]-6-fluorospiro[isoquinoline-4(1*H*),3′-pyrrolidine]-1,2′,3,5′(2*H*)-tetrone and Congeners. 1

Michael S. Malamas,*,† Thomas C. Hohman,‡ and Jane Millen‡,§

Wyeth-Ayerst Research, Inc., CN 8000, Princeton, New Jersey 08543-8000

Received January 11, 1994®

The high concentrations of plasma glucose formed during diabetic hyperglycemia rapidly translate into high levels of glucose in tissues where glucose uptake is independent of insulin. In these tissues that include the lens, retina, nerve, and kidney, this excess glucose enters the sorbitol (polyol) pathway. The first enzyme in this pathway, aldose reductase, reduces glucose to sorbitol. The diabetes-induced increased flux of glucose through the polyol pathway is believed to play an important role in the development of certain chronic complications of diabetes mellitus. Compounds that inhibit aldose reductase activity and block the flux of glucose through the polyol pathway prevent the development of neuropathy and nephropathy in diabetic animals and interrupt the progression of neuropathy in diabetic patients. Here we describe the preparation and characterization of novel aldose reductase inhibitors. These spiro[isoquinoline-4(1*H*),3′-pyrrolidine]-1,2′,3,5′-(2*H*)-tetrones, based on the isoquinoline-1,3-dione framework, were evaluated *in vitro* for their ability to inhibit glyceraldehyde reduction, using a partially purified bovine lens aldose reductase preparation, and *in vivo* for their ability to inhibit galactitol accumulation in the lens and sciatic nerve of galactose-fed rats. Substitution at the N-2 position of the isoquinoline-1,3-dione framework with diverse structural substituents (i.e., aralkyl, benzothiazolylmethyl, methyl) produced several excellent series of ARIs. Optimization of these new series of spirosuccinimides through structure–activity relationship (SAR) studies, including analogy from other drug series (ponalrestat, zopolrestat), led to the design of the clinical candidate 2-[(4-bromo-2-fluorophenyl)methyl]-6-fluorospiro[isoquinoline-4(1*H*),3′-pyrrolidine]-1,2′,3,5′(2*H*)-tetrone (**41**). Compound **41** exhibited exceptional oral potency in two animal models of diabetic complications, the 14-day galactose-fed and streptozocin-induced diabetic rats, with ED_{50} values for the sciatic nerve of 0.1 and 0.09 mg/kg/day, respectively. Both enantiomeric forms of **41** exhibited similar inhibitory activity in both *in vitro* and *in vivo* assays possibly due to their rapid interconversion. In an *ex vivo* experiment, the pharmacodynamic effect of **41** in the plasma of rats and dogs, after a single dose, appeared to be comparable to that of tolrestat.

Introduction

Advances in the treatment of diabetes mellitus have resulted in a longer life expectancy for diabetic patients. This longer survival, however, has been accompanied by an increased probability for the development of complications secondary to the chronic hyperglycemia often associated with diabetes mellitus.[1,2] Two of the most common complications are diabetic peripheral sensorimotor polyneuropathy and diabetic autonomic neuropathy.[3] Peripheral neuropathy is a significant contributing factor in the development of foot ulcers, which may lead to amputation or death by septic shock. Autonomic neuropathy also causes morbidity, placing a diabetic patient at higher risk for cardiac failure, a significant cause of death among diabetics.

The clinical problems of the patient with diabetic neuropathy stem from the abnormal metabolic, functional, and morphological state of the patient's nerve. These include the loss of sensation in the extremities, pain, paresthesia, weakness in the foot muscles leading to Charcot's foot, hypotension, and other diminished cardiovascular reflexes.

Existing treatment of diabetic neuropathy is symptomatic. Tricyclic antidepressants have relieved symptoms in some patients, but these agents do not reverse or inhibit the underlying metabolic, morphologic, and functional damage. Studies examining the advantages of rigorous control of blood glucose have demonstrated that intensive insulin therapy reduces the rate of development of complications.[4] Treatments that attempt to rigorously control blood glucose, however, possess a substantial increased risk of hypoglycemia compared to conventional therapy and are also unavailable to many patients.[5,6] Aldose reductase inhibitors are a new class of compounds that have a considerable potential for the treatment of this disease, without increased risk of hypoglycemia.[7,8]

The probability of a diabetic patient developing neuropathy is directly correlated with the duration of diabetes and the severity of hyperglycemia.[1,3] Diabetic hyperglycemia substantially alters nerve metabolism. Since glucose entry into nerve cells is independent of insulin, during diabetic hyperglycemia the level of glucose in the nerve rapidly increases until it equilibrates with the level of glucose in the plasma. The excess glucose in the nerve is metabolized, in part, by the polyol pathway. Compelling evidence from animal studies[7,9–12] and recent results from

† Department of Medicinal Chemistry.
‡ Department of Experimental Therapeutics.
§ Present address: School of Pharmacy, University of North Carolina, Chapel Hill, NC 27599-7360.
® Abstract published in *Advance ACS Abstracts*, May 1, 1994.

0022-2623/94/1837-2043$04.50/0

clinical studies[13-17] have implicated the diabetes-induced increased flux of glucose through the polyol pathway in the initiation of the secondary complications of diabetes. The first enzyme in the polyol pathway, aldose reductase, catalyzes the NADPH-dependent (nicotinamide adenine dinucleotide phosphate, reduced form) reduction of glucose to sorbitol. The second enzyme in the pathway, sorbitol dehydrogenase, converts sorbitol to fructose, at the expense of NAD (nicotinamide adenine dinucleotide).

The increased flux of glucose through the polyol pathway perturbs membrane transport processes, upsets the cellular redox potential, and initiates a cascade of events that result in the development of diabetic neuropathy, retinopathy, nephropathy, and cataract formation.[7,18,19] Aldose reductase inhibitors (ARIs), compounds which block the flux of glucose through the polyol pathway, prevent the development of these complications in animals[9-12] and halt the progression of diabetic neuropathy and stimulate nerve repair in humans.[13-17]

Since aldose reductase inhibitors inhibit the pathogenesis of diabetic complications at a point after hyperglycemia, they do not pose the risk of hypoglycemia.[7] Additionally, because these compounds have no effect on plasma glucose levels, they can be used as an adjuvant to therapies that attempt to rigorously control blood glucose.

Clinical experience has been reported for a number of aldose reductase inhibitors, most notably tolrestat, sorbinil, ponalrestat, epalrestat, imirestat, and ADN-138.[13-17,20-38] Tolrestat has been shown to improve nerve ultrastructure and function after long-term treatment and is currently approved for marketing in several countries.[13-17,28,38] Epalrestat is currently approved for marketing in Japan. Although sorbinil treatment improved both the structure and function of nerves in diabetic neuropathic patients, it was withdrawn from clinical trials because of toxicity.[15,24,39] Ponalrestat, imirestat, and ADN-138 have also been withdrawn from clinical trials due to toxicity or lack of efficacy.

Orally active ARIs are limited for the most part to two classes, the carboxylic acids and the cyclic imides[21-24,40,41] (Chart 1). Even though both series have similar intrinsic activity for the isolated aldose reductase, their *in vivo* potencies are quite different. *In vitro*, both series reduce aldose reductase activity by 50% at approximately 10^{-8} M concentrations.[40,41] *In vivo*, in the 4-day galactosemic rat animal model, the carboxylic acids reduce polyol accumulation in the sciatic nerve by 50% at doses ranging from 3.0 to 15.0 mg/kg/day, while the imides require only 0.1–0.5 mg/kg/day for the same response.[40,41] The increased potency of the imide type ARIs is possibly due to better pharmacokinetic properties, including absorption and tissue penetration. As a follow on to tolrestat (1), one of the most effective ARIs within the carboxylic acid series, our goal was to identify a structurally novel ARI with much greater potency than that of tolrestat. Our efforts were focused within the imide-type ARIs. On the basis of the reported literature[23,24,40,41] for this class of compounds, and using imides 11 and 13 as templates, we were able to design a structurally novel isoquinolinedione framework (Chart 2) which served as the backbone for the production of several new series of ARIs. Chart 2 outlines the diversity of the new isoquinolinedione backbone which led to the discovery of a large variety of ARIs including spirosuccinimides, spirolactams, spiropyridazines, and carboxylic acid compounds. Substitution positions 2 and 4 of the isoquinoline backbone were very important for the design of these inhibitors. Incorporation of either a pyrrolidine ring, an azetidine ring, a pyridazine ring, or an acetic acid moiety at the more critical 4-position has generated structurally diverse ARIs (15–19). Small groups (i.e., methyl) or even bulkier groups (i.e., aralkyl) were accommodated very well at the 2-position without causing a significant loss in activity.

This paper will focus on the spirosuccinimide series (15, Chart 2), one of the most potent series of the cyclic imide-type ARIs reported to date, which led to the discovery of our new clinical candidate 2-[(4-bromo-2-fluorophenyl)-methyl]-6-fluorospiro[isoquinoline-4(1*H*),3′-pyrrolidine]-1,2′,3,5′(2*H*)-tetrone (41). In a subsequent paper we will report our findings with the other series 16–19.

Chart 1

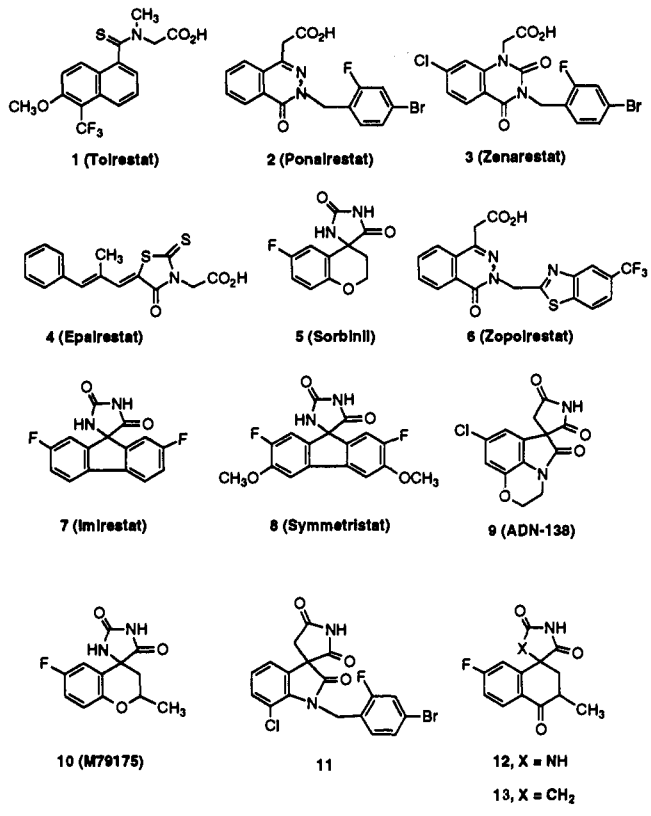

Chart 2

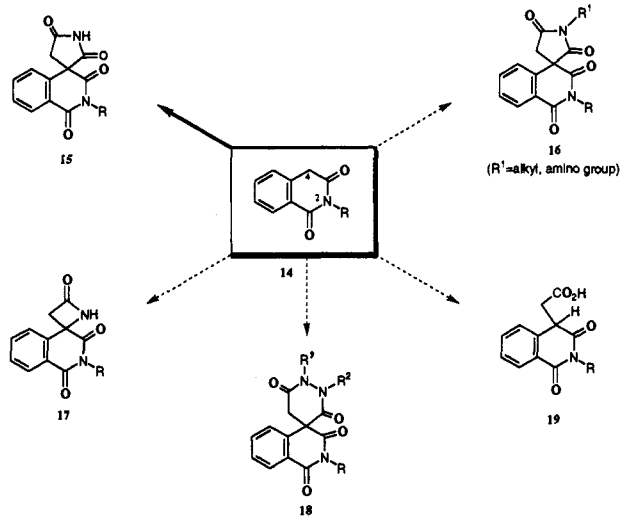

Scheme 1[a]

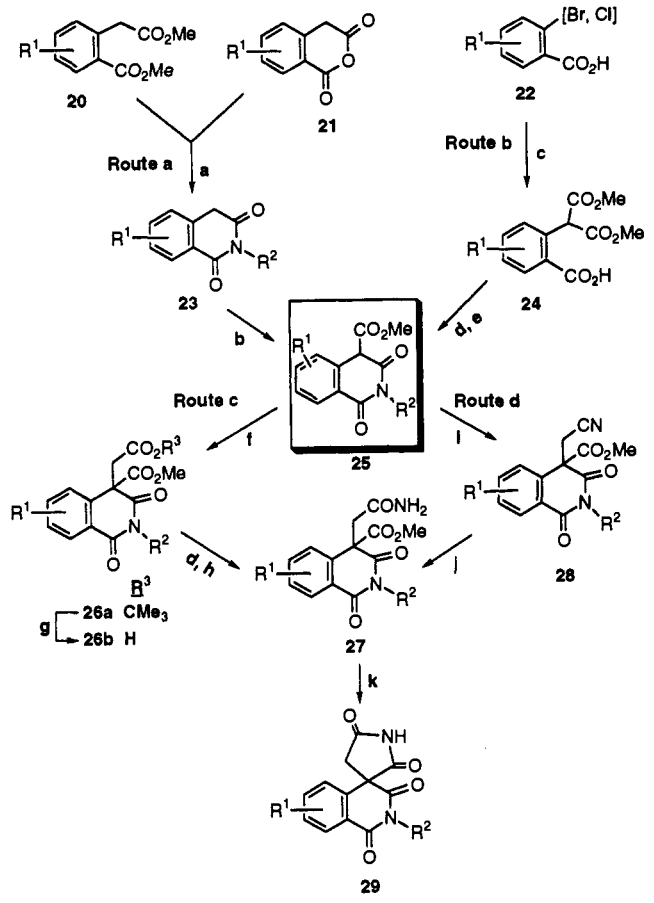

[a] Reagents: (a) R^2NH_2, DMF or xylenes (R^2 = aralkyl or alkyl); (b) $CNCO_2Me$, $LiN(SiMe_3)_2$, THF; (c) $CH_2(CO_2Me)_2$, NaH, CuBr; (d) $SOCl_2$; (e) R^2NH_2, THF (R^2 = aralkyl, alkyl); (f) $BrCH_2CO_2CMe_3$, K_2CO_3; (g) CF_3CO_2H, CH_2Cl_2; (h) NH_3(g), THF; (i) $BrCH_2CN$, K_2CO_3; (j) MeOH, Et_2O, HCl(g); (k) NaH or $LiN(SiMe_3)_2$, or NaOMe.

Scheme 2[a]

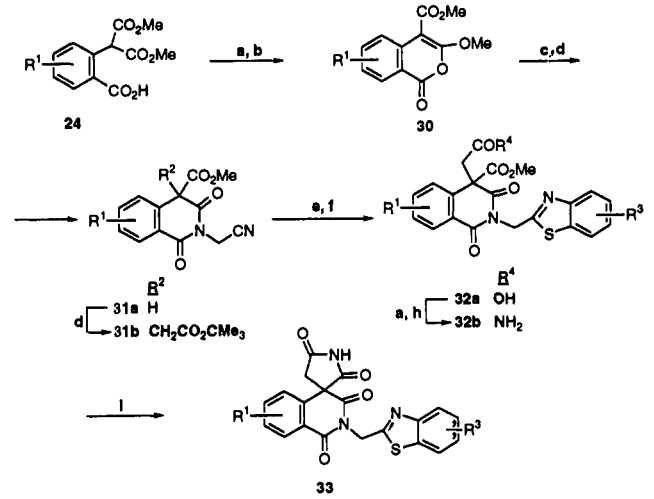

[a] Reagents: (a) $SOCl_2$; (b) Et_3N, THF; (c) $H_2NCH_2CN{\cdot}HCl$, Et_3N, DMF; (d) $BrCH_2CO_2CMe_3$, K_2CO_3; (e) 2-aminothiophenol (R^3 = 5-H or 5-CF3); (f) CF_3CO_2H, CH_2Cl_2; (h) NH_3(g), THF; (i) NaH, DMF.

Chemistry

The spiro[isoquinoline-4(1*H*),3′-pyrrolidine]-1,2′,3,5′-(2*H*)-tetrones (Tables 1–3) were prepared by the general synthetic Schemes 1 and 2. In Scheme 1, a key advanced intermediate **25** was utilized for the preparation of compounds shown on Tables 1 and 2. This intermediate **25** was prepared by two synthetic routes, a and b. In route a, commercially available homophthalic acid diester **20** or homophthalic anhydride **21** was reacted with the required amine (alkyl- or aralkylamine) to give homophthalimide **23**. Treatment of **23** with Mander's reagent[42] yielded the key intermediate **25**. In route b, ortho-halogenated benzoic acid **22** was converted to diester **24** by the Hurtley reaction.[43] Treatment of **24** with thionyl chloride and further reaction of the generated acid chloride with the appropriate amine gave the key intermediate **25**. Conversion of **25** to the final product was accomplished by routes c and d. In route c, alkylation of **25** with *tert*-butyl bromoacetate followed by acidic hydrolysis gave acid **26b**. Generation of the acid chloride of **26b** with thionyl chloride and treatment with ammonia yielded amide **27**. In route d, amide **27** was obtained in a more direct way, by formation of nitrile **28** from **25** with bromoacetonitrile and subsequent acidic hydrolysis. Amide **27** was cyclized to the final product **29**, upon treatment with a variety of bases [sodium hydride, sodium methoxide, lithium bis(trimethylsilyl)-amide].

Scheme 2 shows the preparation of the compounds in Table 3. Diester **24** was first converted to benzopyran **30**, which upon treatment with aminoacetonitrile gave nitrile **31a**. Alkylation of **31a** with *tert*-butyl bromoacetate followed by benzothiazole formation and acidic hydrolysis, produced acid **32a**. Compound **32a** was converted to the final product **33** in a similar manner as described in Scheme 1.

Preparation of the Enantiomers. The enantiomers of the spiro[isoquinoline-4(1*H*), 3′-pyrrolidine]-1,2′,3,5′-(2*H*)-tetrones were obtained by separation of diastereomeric intermediates. The preparation of the enantiomers of **40** and **41** (Table 1) is outlined in Scheme 3. Homophthalimide **34** (prepared according to Scheme 1) was treated with (−)-menthyl chloroformate, followed by alkylation with *tert*-butyl bromoacetate to give a mixture of two diastereomers **35b**. High-pressure liquid chromatographic separation of mixture **35b** yielded diastereomers **36a** and **37a** in greater than 99.5 diastereomeric excess. Each diastereomer was further converted to the final products **38** and **39** by a similar manner as described in Scheme 1. The final cyclization of this process was accomplished with lithium or sodium bis(trimethylsilyl)-amide as the base, in THF at low temperatures (−78 °C). Both products were obtained in greater than 99.5 enantiomeric excess. Higher temperatures or more polar solvents resulted in an extensive racemization of the final products. The absolute configuration of the enantiomers was determined by single-crystal X-ray analyses of enantiomers **82** and **83** (Table 7, Figure 1). The *n* refined value from the X-ray analysis of **82**, the negatively rotating enantiomer of **40**, was 1.04 for the structure with C(4)(*S*) stereochemistry, suggesting this to be the absolute stereochemistry. The *n* refined value for **83**, the positively rotating enantiomer of **41**, was found to be zero for the structure with C(4)(*R*) stereochemistry. Since **83** differs from **82** only by a fluorine atom at the 6-position, its absolute configuration, assigned by comparison to **82**, was C(4)(*R*).

Results and Discussion

The test compounds were evaluated for their *in vitro* inhibitory activity against bovine lens aldose reductase with DL-glyceraldehyde as the substrate.[44] The *in vitro* activity was expressed either as the concentration of the

Table 1. Chemical and Biological Data of Aralkyl N-2 Substituted Spiro[isoquinoline-4(1*H*),3′-pyrrolidine]-1,2′,3,5′(2*H*)-tetrones[g]

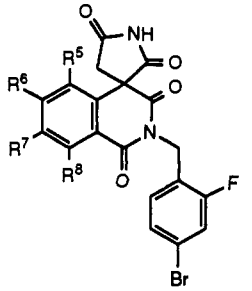

compd	R^5	R^6	R^7	R^8	inhibition of aldose reductase *in vitro*[a] IC_{50}, 10^{-8} M	dose, mg/kg/day	% inhibition of galactitol accumulation *in vivo*[c] sciatic nerve[b]	mp, °C
40	H	H	H	H	2.3	0.5	82 ± 4.0	175–176
41	H	F	H	H	1.4	0.5	83 ± 5.4	232–233
42	F	H	H	H	2.1	0.5	52 ± 6.7	202–203
43	H	H	F	H	2.0	1.0	50 ± 10	189–190
44	H	H	H	F	2.3	0.5	51 ± 6.5	127–129
45	H	H	Cl	H	3.3	0.6	63 ± 6.7	187–188
46	H	Cl	H	H	3.0	0.6	29 ± 11.3[d]	196–197
47	H	Br	OCH_3	H	2.8	0.5	55 ± 4.6	134–136
48	F	OCH_3	H	H	3.0	0.5	43 ± 13	232–233
49	H	H	OCH_3	H	3.7	25.6	88 ± 2.4	160–161
50	H	CF_3	H	H	3.8	1.0	26 ± 6.3	106–107

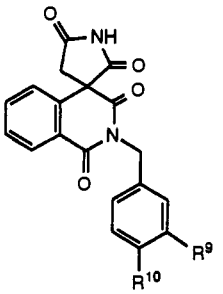

compd	R^9	R^{10}	inhibition of aldose reductase *in vitro*[a] IC_{50}, 10^{-8} M	dose, mg/kg/day	% inhibition of galactitol accumulation *in vivo*[c] sciatic nerve[b]	mp, °C
51	H	Br	2.2	1.0	50 ± 13	137–138
52	Cl	Cl	2.2	1.1	64 ± 2.79	118–120
53	H	Cl	2.2	1.0	NS[e]	142–144
54	H	CF_3	2.5	10.6	NS	163–164
55	H	OCH_3	2.5	10.5	NS	145–147
56	CH_3	H	2.5	10.2	NS	168–169
57	CF_3	H	1.7	10.3	NS	115–116
totrestat			3.3 ± 0.2[f]		ED_{50} = 6.4 ± 0.8 mg/kg/day[f]	

[a] Inhibition of enzymatic activity in a partially purified bovine lens preparation. [b] Inhibition of galactitol accumulation in the sciatic nerves of rats fed 20% galactose for 4 days; compounds were administered in the diet; compounds **40–57** were inactive or very weakly active in the lens at the given doses. [c] Values are mean ±SEM; mean of six animals; $p < 0.01$ unless indicated. [d] $p < 0.05$. [e] NS = no significant inhibition of polyol accumulation. [f] Values are mean of nine separate determinations with 95% confidence interval. [g] All compounds were prepared according to the synthetic Scheme 1.

test compound which inhibited enzyme activity by 50% (IC_{50}) or the average inhibition of the test compound at 1×10^{-5}, 1×10^{-6}, 1×10^{-7}, and 4×10^{-8} M concentrations.

In vivo, the test compounds were evaluated for their ability to inhibit either galactitol or sorbitol formation in the sciatic nerve and lens of galactosemic or streptozocin-induced diabetic rats, respectively.[45] The *in vivo* activity was expressed as the daily dose, in milligrams per kilogram, that produced a specified decrease in tissue polyol levels. The ED_{50} value of several compounds was calculated and represents the dose causing 50% decrease in polyol accumulation. Tolrestat was the reference standard in all of the assays.

Results with the spiro[isoquinoline-4(1*H*),3′-pyrrolidine]-1,2′,3,5′(2*H*)-tetrones, substituted at the N-2 position with the 4-bromo-2-fluorobenzyl moiety, are shown in Table 1. Britain and co-workers first introduced this moiety in ponalrestat[46] and demonstrated that it very effectively enhanced oral potency of this compound. Substitution of the fused benzene ring of the isoquinoline ring (Table 1) with either electron-withdrawing groups (i.e., halogens) or electron-donating groups (i.e., methoxy) did not have a significant effect on the *in vitro* activity and produced only modest differences in their *in vivo* potency. While analogous substitutions on the benzyl moiety (Table 1) had no effect on the intrinsic activity, these modifications resulted in considerable loss of oral activity (**54–57**). Undesirable pharmacokinetics, i.e., poor absorption, poor tissue penetration, and/or short half-life, may have contributed to the decreased *in vivo* activity.

Results for the series of compounds in which the benzothiazolylmethyl moiety was introduced at the N-2

Table 2. Chemical and Biological Data of 2-(Benzothiazolylmethyl)spiro[isoquinoline-4(1*H*)-3′-pyrrolidine]-1,2′,3,5′(2*H*)-tetrones[d]

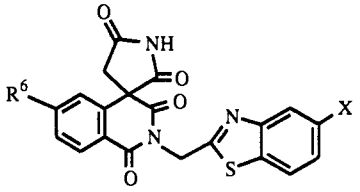

compd	R^6	X	inhibition of aldose reductase *in vitro*[a] IC_{50}, 10^{-8} M	dose, mg/kg/day	% inhibition of galactitol accumulation *in vivo*[c] sciatic nerve[b]	mp, °C
77	H	H	1.5	1.1	50 ± 12	225–227
78	H	CF_3	2.2	0.5	49 ± 5.2	122–124
79	F	H	1.8	4.6	63 ± 5.6	198–199
80	F	CF_3	2.6	1.0	53 ± 18	123–125

[a] Inhibition of enzymatic activity in a partially purified bovine lens preparation. [b] Inhibition of galactitol accumulation in the sciatic nerves of rats fed 20% galactose for 4 days; compounds were administered in the diet; compounds 77–80 were inactive or very weakly active in the lens at the given doses. [c] Values are mean ± SEM; mean of six animals; $p < 0.01$. [d] All compounds were prepared according to the synthetic Scheme 2.

Table 3. Chemical and Biological Data of 2-Alkyl- or 2-Alkoxyspiro[isoquinoline-4(1*H*),3′-pyrrolidine]-1,2′,3,5′(2*H*)-tetrones[h]

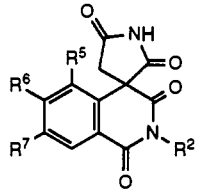

compd	R^2	R^5	R^6	R^7	% inhibition of aldose reductase *in vitro*[a] 10^{-7} M	% inhibition of aldose reductase *in vitro*[a] 4×10^{-8} M	dose, mg/kg/day	% inhibition of galactitol accumulation *in vivo*[c] lens[b]	% inhibition of galactitol accumulation *in vivo*[c] sciatic nerve[b]	mp, °C
58	CH_3	H	H	H	63	38	1.0	15 ± 13	37 ± 9.3	224–225
							3.0	43 ± 2.8	66 ± 4.1	
59	CH_2CH_3	H	H	H	27	17	11.0	NS[e]	NS	183–185
60	$(CH_2)_2CH_3$	H	H	H	19	NS[g]	11.0	NS	NS	190–192
61	$(CH_2)_3CH_3$	H	H	H	17	19	10.0	NS	NS	143–144
62	CH_3	H	Cl	H	72	43	0.5	NS	54 ± 2.1	236–237
							1.1	33 ± 4.9	75 ± 4.3	
							3.0	59 ± 4.8	75 ± 4.2	
63	CH_3	H	H	Cl	61	34	3.0	NS	NS	234–236
64	CH_3	Cl	H	H	24	11	1.1	NS	NS	285–287
65	CH_3	H	F	H	74	36	1.0	NS	NS	225–226
66	CH_3	H	Br	H	85	43	1.0	NS	54 ± 6.9[d]	247–248
67	CH_3	H	CF_3	H	64	46	0.9	20 ± 2.8	38 ± 7.2	214–215
68	CH_3	H	Cl	OCH_3	84	66	0.5	NS	51 ± 6.5	242–243
69	CH_3	H	NO_2	H	71	53	0.9	NS	NS	193–194
70	CH_3	H	Cl	Cl	89	84	0.9	NS	NS	162–164
71	CH_3	H	CH_3	H	65	35	0.9	NS	NS	202–203
72	CH_3	H	OCH_3	H	63	30	1.0	NS	NS	222–223
73	CH_3	H	OCH_3	Br	17	NS	1.0	NS	NS	259–260
74	CH_3	H	H	OCH_3	55	41	1.1	NS	NS	159–160
75	OCH_3	H	H	H	NS	NS		ND[f]	ND	203–205
76	OCH_3	H	Cl	H	27	11	9.6	NS	NS	125–127

[a] Inhibition of enzymatic activity in a partially purified bovine lens preparation. [b] Inhibition of galactitol accumulation in the sciatic nerves or lenses of rats fed 20% galactose for 4 days; compounds were administered in the diet. [c] Values are mean ± SEM; mean of six animals; $p < 0.01$, unless indicated. [d] $p < 0.05$. [e] NS = no significant inhibition of polyol accumulation. [f] ND = not determined. [g] No significant inhibitory activity at the given concentration. [h] All compounds were prepared according to the synthetic Scheme 1.

position of the isoquinoline ring are shown in Table 2. Mylari and co-workers have demonstrated that the 4-bromo-2-fluorobenzyl group found in ponalrestat can be replaced by the [5-(trifluoromethyl)benzothiazolyl]-methyl moiety and generate a new ARI (zopolrestat),[47] equipotent to ponalrestat. Similarly to the phthalazinone series (ponalrestat, zopolrestat), incorporation of the benzothiazolylmethyl moiety into our isoquinolinedione framework has generated ARIs **77–80** that are highly potent upon oral administration (Table 2). In contrast to the zopolrestat series where the [5-(trifluoromethyl)-substituted benzothiazolyl]methyl group was superior to the unsubstituted analogue,[47] the corresponding analogues within our series appear to be equipotent (**77** vs **78**).

Results for compounds in which alkyl and alkoxy substituents were introduced at the N-2 position of the isoquinoline ring are shown in Table 3. Methyl substitution at the N-2 position produced very potent aldose reductase inhibitors while bulkier alkyl groups or alkoxy substituents resulted in a loss of the activity (**58** vs **59–61**, **75**). Substitution of the fused benzene ring was also critical to both *in vitro* and *in vivo* activity. Electron-withdrawing groups (i.e., halogens) at position 6 produced the most potent inhibitors. Similar substitution at this position was also shown to be preferable for sorbinil and its analogs.[24,41] Halogen substitution at position 5 was found to be detrimental to the activity (**64** vs **62**), possibly due to the steric interference caused by the close vicinity of

Scheme 3[a]

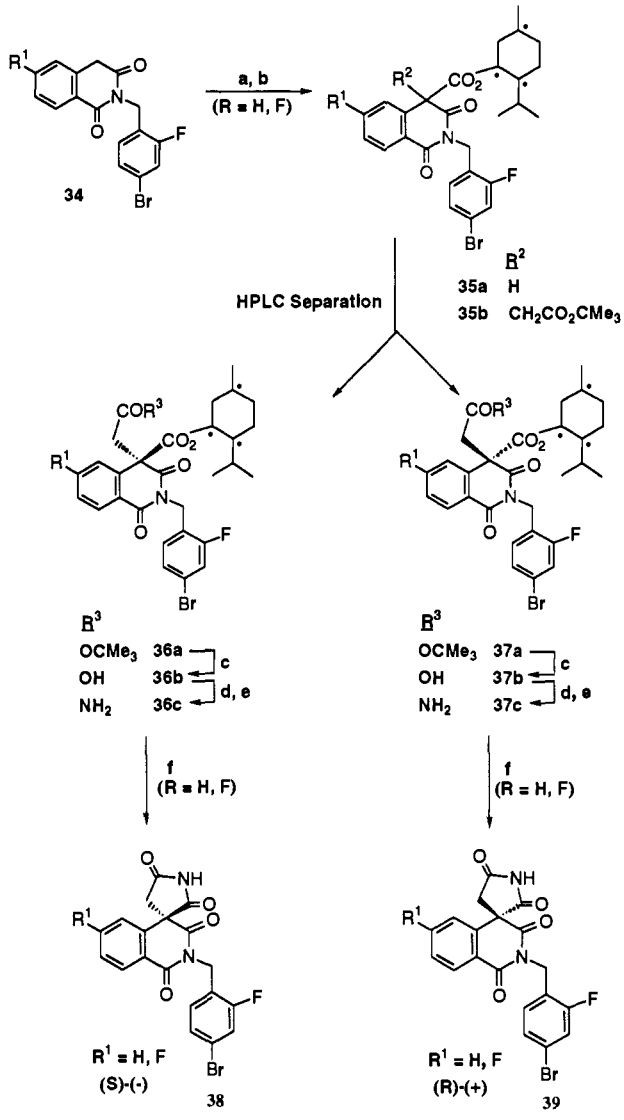

[a] Reagents: (a) (−)-menthyl chloroformate, LiN(SiMe3)2, THF; (b) BrCH2CO2CMe3, K2CO3; (c) CF3CO2H, CH2Cl2; (d) SOCl2; (e) NH3(g), THF; (f) LiN(SiMe3)2, THF.

the chlorine group to the spiropyrrolidine ring. Electron-donating groups (i.e., alkoxy) at either position 6 or 7 caused only marginal decreases in inhibitory activity (**72** vs **74**). However, results with the disubstituted 6,7-alkoxy/halogen analogs **68** and **73** were quite different. Compound **68** retained its inhibitory activity while **73** was found to be inactive. *In vivo*, the monosubstituted 6-chloro and 6-bromo analogs **62** and **66** and the disubstituted 6-chloro-7-methoxy analog **68** were found to be the most potent oral inhibitors. The unsubstituted analog **58** and the 6-CF_3 analog **67** were also active, but less potent.

These biological results (Tables 1–3) indicate that the N-2 position of the isoquinolinedione backbone of these inhibitors can accommodate a diverse array of different substituents (i.e., dihalogenated aralkyl, benzothiazolylmethyl, methyl) to produce inhibitors with excellent oral potency.

Lipophilicity and Oral Potency. The lipophilic nature of the spiro[isoquinoline-4(1*H*),3′-pyrrolidine]-1,2′,3,5′(2*H*)-tetrones appears to play an important role in the inhibition of polyol accumulation in the lens (Table 4). Compounds with low log *p* values (i.e., **58**, **62**) have shown higher inhibitory potency in the lens than the more lipophilic inhibitors (i.e., **40**, **41**). Since the lens is avascular and is surrounded by an aqueous barrier, the aqueous humor, orally administered compounds upon entering systemic circulation have to cross the blood–aqueous humor barrier to reach the lens. Drug transport from the blood to the lens is favored for compounds with low log *p* values (hydrophilic). Lipophilicity appears to be less critical to inhibition of polyol accumulation in the sciatic nerve (Table 4). Compound **62**, with log *p* = 0.58, is equipotent to the more lipophilic compounds **40**, **41**, **45**, **52**, **78**, **80**, with log *p* values in the range 2.74–3.51.

Preclinical Evaluation of 41. Compound **41** was further evaluated in two animal models of diabetic complications, the STZ diabetic and galactosemic rats. *In vitro* and *in vivo* pharmacology and pharmacokinetics in rats and dogs compared **41** versus its desfluoro analog **40** and tolrestat (**1**) in order to assess its biological profile prior to clinical evaluation. Results of these studies are presented below. The intrinsic activities of these three ARIs were assessed in two *in vitro* assays, first with partially purified bovine lens aldose reductase and second with isolated whole RBCs incubated in medium containing galactose. RBCs of rats and dogs were used in the second *in vitro* assay. In both of the *in vitro* assays (Tables 1 and 5), these three inhibitors exhibited similar intrinsic activity. AR activity was reduced by 50% at concentrations of approximately 10^{-8} M.

These inhibitors were evaluated *in vivo* for their ability to block tissue polyol accumulation in diabetic and galactosemic rats. In animal studies examining the role of aldose reductase in the development of diabetic complications, galactose-fed rats are a frequently used model. Since aldose reductase has a 4-fold greater affinity for galactose than glucose, the polyol insult leading to diabetic complications is significantly greater in the galactocemic than the diabetic rat model.[48] In the 14-day streptozocin-induced diabetic rat model, both **40** and **41** were superior to tolrestat with ED_{50} values of 0.07 and 0.09 mg/kg/day, respectively, versus 3.8 mg/kg/day for tolrestat (Table 6). Compound **41** was further evaluated in two additional tissues, the lens and the RBC, and was found to effectively inhibit polyol accumulation in these tissues at very low oral doses, with ED_{50} values of 0.4 mg/kg/day for the lens and 0.25 mg/kg/day for the RBC (Table 6). In the 4-day galactose-fed rat model, **40** and **41** were also superior to tolrestat, reducing polyol accumulation in the sciatic nerve with ED_{50} values of 0.3 mg/kg/day and in the lens with ED_{50} values of 10–19 mg/kg/day (Table 6). In a longer experiment, where rats were fed galactose and **41** for 14 days, the ED_{50} value for the sciatic nerve was not significantly decreased, while the ED_{50} value in the lens was decreased about 5-fold (Table 6). The apparent decreased lens potency in 4-day galactosemic rats may be due to the duration of the assays. Four days may not be sufficient time to allow maximum drug penetration in all of the target tissues. Similar observations have been reported for tolrestat.[49]

The effects of **41** on the reaction kinetics of the enzyme was assessed. A comparison of the initial rates of reduction of glyceraldehyde (substrate) by bovine lens aldose reductase in the absence or presence of varying concentrations of **41**, as well as varying concentrations of glyceraldehyde (Figure 2) and NADPH (data not shown), indicates that compound **41** is a reversible, mixed type uncompetitive/noncompetitive inhibitor.

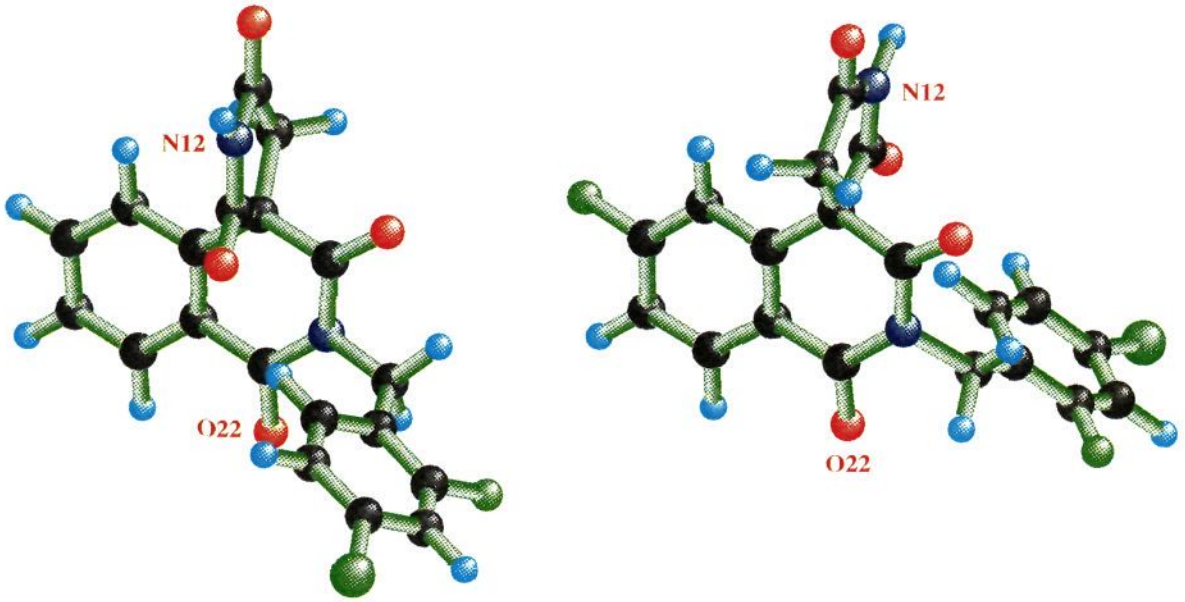

Figure 1. X-ray structure of **82** (left) and **83** (right).

Table 4. Lipophilicity and Oral Potency of the Spiro[isoquinoline-4(1*H*),3′-pyrrolidine]-1,2′,3,5′(2*H*)-tetrones

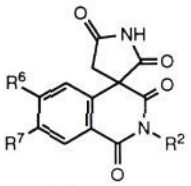

compd	R^2 [a]	R^6	R^7	log p [b]	dose, mg/kg/day	% inhibition of galactitol accumulation *in vivo* [d] lens [c]	% inhibition of galactitol accumulation *in vivo* [d] sciatic nerve [c]
40	A	H	H	2.74	0.8	NS [e]	88 ± 5.1
					3.1	27 ± 1.7	92 ± 3.7
41	A	F	H	2.82	1.1	NS	95 ± 2.1
					4.0	NS	94 ± 0.5
45	A	H	Cl	3.51	0.6	NS	63 ± 6.7
52	B	H	H	3.09	1.0	NS	64 ± 2.79
					3.0	NS	76 ± 3.2
78	C	H	H	3.17	0.5	NS	49 ± 5.2
					1.1	22 ± 6.1	100 ± 17
80	C	F	H	3.16	1.0	NS	53 ± 18
58	CH_3	H	H	0.24	1.0	15 ± 1.3	37 ± 9.3
					3.0	43 ± 2.8	66 ± 4.1
62	CH_3	Cl	H	0.58	1.1	33 ± 4.9	75 ± 4.3
					3.0	59 ± 4.8	75 ± 4.2
66	CH_3	Br	H	0.8	1.0	NS	54 ± 6.9

[a] A = 4-Br-2-F$C_6H_3CH_2$; B = 3,4-$Cl_2C_6H_3CH_2$; C = 5-CF_3 benzothiazolylmethyl. [b] Octanol/pH 7.4 buffer. [c] Inhibition of galactitol accumulation in the sciatic nerves or lenses of rats fed 20% galactose for 4 days; compounds were administered in the diet. [d] Values are mean ± SEM; mean of six animals; $p < 0.01$. [e] NS = no significant inhibition of polyol accumulation.

Other ARIs that can be isolated into isomeric forms have shown high enantioselectivity for the aldose reductase binding site. The enantioselectivity for the AR binding site of the enantiomers of **40** and **41** was determined *in vitro* and *in vivo*. *In vitro*, the positively rotating enantiomer (**81**) of **40** demonstrated high enantioselectivity for the AR binding site. It was found to be 100 times more potent than the negatively rotating enantiomer **82** (Table 7). Differences in the intrinsic activity of these enantiomers were reflected in the results of the *in vivo* assay (Table 7). At a dose of 0.5 mg/kg in the 4-day galactosemic rat assay, the (+)-enantiomer **81** and the racemate **40** were

Table 5. *In Vitro* Inhibitory Activity of **40**, **41**, and Tolrestat

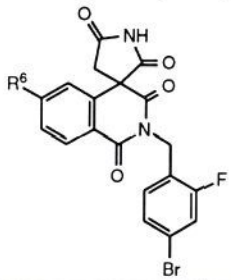

compd	R^6	IC_{50}, 10^{-8} M [a] rat RBC	IC_{50}, 10^{-8} M [a] dog RBC
40	H	–	1.94 ± 0.56
41	F	2.69 ± 0.75	1.22 ± 0.25
tolrestat		2.72 ± 0.07	2.39 ± 0.33

[a] Concentration which inhibits aldose reductase activity by 50%; mean ± SD from three to six replicate experiments.

nearly equipotent in the sciatic nerve, while the (−)-enantiomer **82** was inactive. The enantiomers of **41** exhibited identical intrinsic activity that was indistinguishable from that of the racemate (Table 7). These results would be expected if **83** and **84** racemize rapidly. *When the enantiomeric half-life was estimated polarimetrically* in dimethyl sulfoxide, both enantiomers **83** and **84** had a half-life of about 20 min. The enantiomers of **40** (**81** and **82**), which were differentiated by their biological activities, had enantiomeric half-lives of 250–350 min (Table 8). Such a unique racemization process of a nonenolizable asymmetric center may be attributed to the facile pyrrolidine ring opening to form the acyl isocyanate (**85**, Chart 3), followed by reclosure. This potential mechanism, which would result in enolization of the C(4) asymmetric center with loss of chirality, is consistent with the enhancement of the racemization process by electron-withdrawing substituents at the 6-position of the isoquinoline ring. The 6-fluoro analogs **83** and **84** racemized much more rapidly than the unsubstituted analogs **81** and **82**.

The pharmacodynamic effect of **41** versus tolrestat (**1**) was assessed *ex vivo* in RBC of rats and dogs. After a

Table 6. *In Vivo* Inhibitory Activity of 40, 41, and Tolrestat

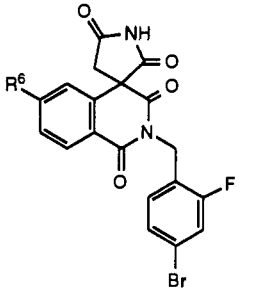

experimental model	compd	R6	ED50, mg/kg/day[a] sciatic nerve	lens	RBC
STZ diabetic rat	40	H	0.07	–	–
14 days	41	F	0.09	0.41	0.25
	tolrestat (1)[b]		3.8	ND	1.9
galactosemic rat	40	H	0.3	~10	–
4 days	41	F	0.3	19	–
	tolrestat (1)[b]		6.4	128	–
14 days	41	F	0.1	4.0	–
12 days	tolrestat (1)[b]		4.5	28	–

[a] Dose at which the tissue level of polyol accumulation was reduced by 50%. [b] Data from refs 7 and 49.

single oral administration of the tested drug, blood samples were collected at selected times. The RBC were isolated and incubated in a galactose medium, and the inhibition of polyol accumulation in the RBC was assessed. In both species as shown in Figure 3, the pharmacodynamic effect decreased with time after a single dose in parallel to the results with tolrestat. For tolrestat the decreasing pharmacodynamic effect paralleled decreasing plasma drug levels,[50] and the half-life of the pharmacodynamic effect was consistent with the reported plasma half-life of 3–4 h in rats and 10–12 h in dogs.[51]

In summary we have identified a novel series of spiro[isoquinoline-4(1*H*),3′-pyrrolidine]-1,2′,3,5′(2*H*)-tetrones as aldose reductase inhibitors with exceptional oral potency. Substitution at the N-2 position of the isoquinolinedione framework with diverse structural substituents (i.e., aralkyl, benzothiazolylmethyl, methyl) has produced several series of excellent AR inhibitors. Lipophilicity appeared to play a more significant role in the inhibition of AR in the lens than in the sciatic nerve. The positively rotating 4*R*-enantiomer 81 has shown higher enantioselectivity for the AR binding site than the negatively rotating 4*S*-enantiomer 82. The C(4) asymmetric center of the 6-F-substituted analog (41) was found to rapidly racemize in polar solvents (DMSO, *in vitro*). In an *ex vivo* experiment, the pharmacodynamic effect of 41 in the plasma of rats and dogs after a single oral dose appeared to be comparable to that of tolrestat.

Experimental Section

Chemistry. Melting points were determined in open capillary tubes on a Thomas-Hoover apparatus, and reported uncorrected ^{1}H NMR spectra were determined in the cited solvent on a Bruker AM 400 (400 MHz), a Varian XL-300 (300 MHz), or a Varian XL-200 (200 MHz) instrument, with tetramethylsilane as an internal standard. Chemical shifts are given in ppm, and coupling constants are in hertz. Splitting patterns are designated as follows: s, singlet; br s, broad singlet; d, doublet; t, triplet; q, quartet; m, multiplet. The infrared spectra were recorded on a Perkin-Elmer 781 spectrophotometer as KBr pellets or as solutions in chloroform. Mass spectra were recorded on either a Finnigan Model 8230 or a Hewlett-Packard Model 5995A spectrometer. Elemental analyses (C, H, N) were performed on a Perkin-Elmer 240 analyzer, and all compounds are within ±0.4% of theory unless otherwise indicated. Optical rotations were determined in the cited solvent on a Perkin-Elmer Model 241 MC polarimeter. All products, unless otherwise noted, were purified by "flash chromatography"[52] with use of 220–400-mesh silica gel. Thin-layer chromatography was done on silica gel 60 F-254 (0.25-mm thickness) plates. Visualization was accomplished with UV light and/or 10% phosphomolybdic acid in ethanol. Unless otherwise noted, all materials were obtained commercially and used without further purification. All reactions were carried out under an atmosphere of dried nitrogen.

General Procedure for the Synthesis of Spiro[isoquinoline-4(1*H*),3′-pyrrolidine]-1,2′,3,5′(2*H*)-tetrones (29, Scheme 1). Compounds of the general structure 29 were synthesized from commercially available, appropriately substituted starting materials by the representative procedures illustrated for analogs 40, 58, and 68 (Tables 1 and 3).

Route a. 2-Methyl-1,3(2*H*,4*H*)-isoquinolinedione (23, R^1 = H, R^2 = Me). Anhydrous monomethylamine was passed through a solution of homophthalic anhydride (10.0 g, 61.73 mmol) in anhydrous THF (200 mL) for 10 min. The formed suspension was stirred for 1 h, and the volatiles were removed in vacuo. The residue was taken in DMF (200 mL), and the suspension was stirred at 180 °C for 10 h. After being cooled to room temperature, the brownish solution was poured into H_2O, extracted with EtOAc,

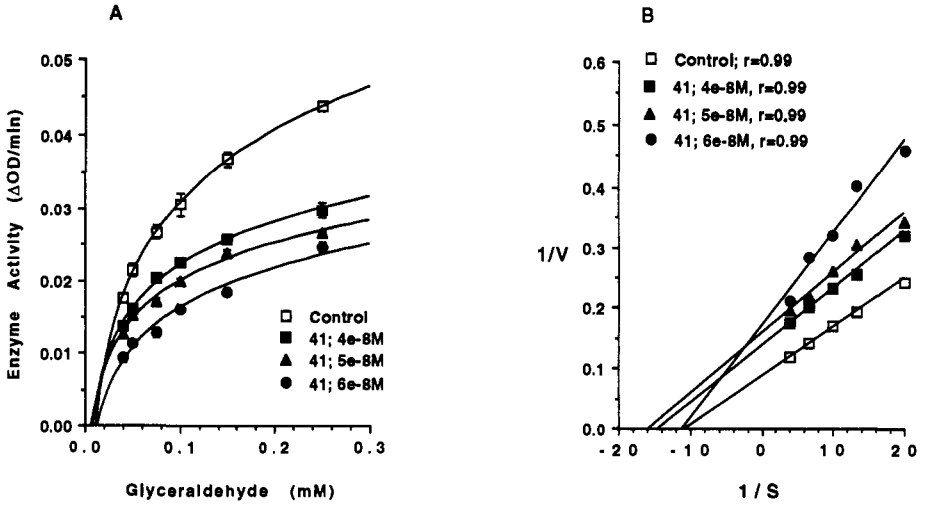

Figure 2. Inhibition of substrate-dependent aldose reductase activity by 41. (A) Aldose reductase activity was quantitated spectrophotometrically by monitoring the rate of NADPH oxidation under conditions where the reaction rate was limited by substrate availability. Each data point is the mean of four replicate observations. (B) Reciprocal plot of the enzyme reaction rate versus substrate concentration.

Table 7. Enantiospecificity of the Spiro[isoquinoline-4(1*H*),3′-pyrrolidine]-1,2′,3,5′(2*H*)-tetrones[a]

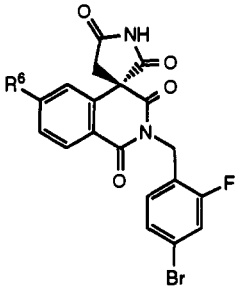

compd	R^6	enantiomer[b]	inhibition of aldose reductase *in vitro*[c] IC_{50}, M	inhibition of galactitol accumulation *in vivo*[e] dose, mg/kg/day	sciatic nerve[d]
40	H	±	2.3×10^{-8}	0.5	76 ± 1.9
81	H	+	9.7×10^{-8}	0.5	83 ± 5.1
82	H	−	1.0×10^{-8}	0.5	NS[f]
41	F	±	1.4×10^{-8}	ED_{50} = 0.09 mg/kg/day[g]	
83	F	+	0.9×10^{-8}	ED_{50} = 0.09 mg/kg/day	
84	F	−	3.2×10^{-8}	ED_{50} = 0.15 mg/kg/day	

[a] The structure shown depicts the absolute configuration of the more active, positively rotating, 4*R* enantiomer; the enantiomers were prepared according to the synthetic Scheme 3. [b] Enantiomeric status "+" = 4*R*; "−" = 4*S*; "±" = racemate. [c] Inhibition of enzymatic activity in partially purified bovine lens preparation. [d] Inhibition of galactitol accumulation in the sciatic nerves of rats fed 20% galactose for 4 days; compounds were administered in the diet. [e] Values are mean ± SEM; mean of six animals; $p < 0.01$. [f] NS = no significant inhibition of polyol accumulation. [g] Inhibition of galactitol accumulation in the sciatic nerves of rats fed 20% galactose for 14 days; compounds were administered in the diet.

Table 8. Enantiomeric Half-Life of the Enantiomers of **40** and **41**

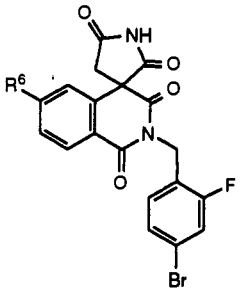

compd	R^6	*in vitro*[a] $t_{1/2}$, h
81	H	4–5
82	H	4–5
83	F	0.5
84	F	0.5

[a] In DMSO.

and dried over $MgSO_4$. The crude product was crystallized from acetone/ether/hexane (after cooling at 0 °C) to yield a yellow solid (7.9 g, 73.1%): mp 120–121 °C; ^{1}H NMR (DMSO-d_6, 400 MHz) δ 3.18 (s, 3H, NCH_3), 4.12 (s, 2H, CH_2CONCH_3), 7.36 (d, J = 7.67 Hz, 1H, Ar-*H*), 7.47 (t, J = 7.37 Hz, 1H, Ar-*H*), 7.64 (t, J = 7.45 Hz, 1H, Ar-*H*), 8.02 (d, J = 7.87 Hz, 1H, Ar-*H*); IR (KBr, cm^{-1}) 1720 (CO), 1665 (CO); MS *m/e* 175 (M^+), 118 (M^+ − $CONCH_3$). Anal. ($C_{10}H_9NO_2$) C, H, N.

6-Chloro-2-methyl-1,3(2*H*,4*H*)-isoquinolinedione (23, R^1 = 6-Cl, R^2 = Me). 5-Chloro-2-(methoxycarbonyl)benzeneacetic acid methyl ester (**20**, R^1 = 6-Cl; 20.0 g, 82.47 mmol) and MeOH (150 mL) were placed in a pressure glass vessel. Anhydrous monomethylamine was passed through the mixture for 30 min. The vessel was introduced into an oil bath and heated at 75 °C for 24 h. After cooling to room temperature, the mixture was poured into H_2O, acidified with HCl (2 N), and extracted with EtOAc. The organic extracts were dried over $MgSO_4$. The crude product was purified by flash chromatography (hexane/EtOAc, 2/1) to yield a yellow solid (11.1 g, 64.2%): mp 167–188 °C; ^{1}H NMR (DMSO-d_6, 200 MHz) δ 3.18 (s, 3H, NCH_3), 4.12 (s, 2H, CH_2CO), 7.52 (m, 2H, Ar-*H*), 8.04 (d, J = 8.8 Hz, 1H, Ar-*H*); IR (KBr, cm^{-1}) 1665 (CO); MS *m/e* 209 (M^+), 152 (M^+ − $CONCH_3$), 124 [M^+ − $CON(CH_3)CO$]. Anal. ($C_{10}H_8ClNO_2$) C, H, N.

1,2,3,4-Tetrahydro-2-methyl-1,3-dioxo-4-isoquinolinecarboxylic Acid Methyl Ester (25, R^1 = H, R^2 = Me). Lithium bis(trimethylsilyl)amide (28.6 mL, 28.6 mmol, 1.0 M in THF) was added dropwise over a 10-min period to a cold (−78 °C) solution of 2-methyl-1,3(2*H*,4*H*)-isoquinolinedione (**23**, R^1 = H, R^2 = Me; 5.0 g, 28.57 mmol) in anhydrous THF (100 mL). After the mixture was stirred for 3 h, methyl cyanoformate (2.76 mL, 34.3 mmol) was added, and the reaction mixture was allowed to warm up to room temperature. The mixture during that period turned a dark color. It was stirred an additional 30 min and quenched with aqueous NH_4Cl. The dark solution was poured into H_2O, acidified with HCl (2 N), and extracted with EtOAc. The organic extracts were dried over $MgSO_4$. The crude product was crystallized from EtOAc/hexane (after cooling to −20 °C) to yield a yellow solid (5.6 g, 84%): mp 130–131 °C; ^{1}H NMR (DMSO-d_6, 200 MHz) δ [3.24 (s), tautomeric, 3H, NCH_3], [3.7 (s), 4.03 (s), tautomeric, 3H, CO_2CH_3], 7.4–8.45 (tautomeric, 4H, Ar-*H*); IR (KBr, cm^{-1}) 3400 (OH), 1670 (CO), 1600 (CO); MS *m/e* 233 (M^+), 118 (M^+ − CO_2Me, − $CONCH_3$). Anal. ($C_{12}H_{11}NO_4$) C, H, N.

Route b. 2-(2-Carboxyphenyl)propanedioic Acid Dimethyl Ester (24, R^1 = H). Sodium hydride (80% in mineral oil; 10.75 g, 358.4 mmol) was added over a 30-min period to a rapidly stirred cold suspension (0 °C) of 2-bromobenzoic acid (30.0 g, 149.3 mmol), cuprous bromide (2.14 g, 14.93 mmol), and dimethyl malonate (300 mL), while a stream of dry N_2 was passed over the mixture. After the addition of the NaH had been completed, the mixture was stirred for 10 min at room temperature and 30 min at 70 °C (external oil bath temperature). At this point, the suspension had turned to a solid mass, which was dissolved in H_2O (1000 mL). The aqueous layer was extracted with diethyl ether (3 × 500 mL) and was then acidified with HCl (2 N). The acidic aqueous layer was extracted with EtOAc. The organic extracts were dried over $MgSO_4$. Evaporation gave an off-white solid which was recrystallized from Et_2O/hexane (after cooling to −20 °C) to give a white solid (**24**, 34.2 g, 90.9%): mp 119–120 °C; ^{1}H NMR (DMSO-d_6, 400 MHz) δ 3.67 [s, 6H, $CH(CO_2CH_3)_2$], 5.72 (s, 1H, $CH(CO_2CH_3)_2$], 7.3 (d, J = 7.76 Hz, 1H, Ar-*H*), 7.45 (dt, J = 7.66, 1.12 Hz, 1H, Ar-*H*), 7.6 (dt, J = 7.66, 1.45 Hz, 1H, Ar-*H*), 7.94 (dd, J = 7.8, 1.33 Hz, 1H, Ar-*H*), 13.2 (s, 1H, CO_2H); IR (KBr, cm^{-1}) 3300–2700 (CO_2H), 1750 (CO), 1730 (CO), 1680 (CO); MS *m/e* 252 (M^+), 220 (M^+ − CH_3OH). Anal. ($C_{12}H_{12}O_6$) C, H.

2-[(4-Bromo-2-fluorophenyl)methyl]-1,2,3,4-tetrahydro-1,3-dioxo-4-isoquinolinecarboxylic Acid Methyl Ester (25, R^1 = H, R^2 = 4-Br-2-$FC_3H_6CH_2$). A mixture of 2-(2-carboxyphenyl)propanedioic acid dimethyl ester (**24**, R^1 = H; 5.0 g, 19.84 mmol) and $SOCl_2$ (20 g) was refluxed for 1.5 h. The volatiles

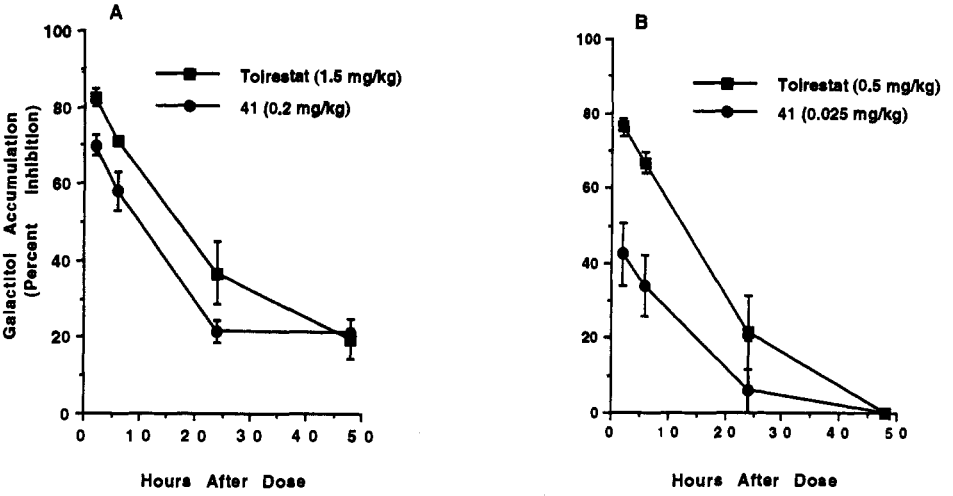

Figure 3. Inhibition of galactitol accumulation in erythrocytes collected from rats (A) or dogs (B) at selected times following the administration of a single dose of tolrestat or 41. Galactitol levels were quantitated in isolated erythrocytes that were incubated in a balanced salt solution enriched with 10 mM galactose for 4 h. Erythrocyte galactitol accumulation in treated animals is expressed as the percent of inhibition in comparison with the results from vehicle-treated animals.

Chart 3

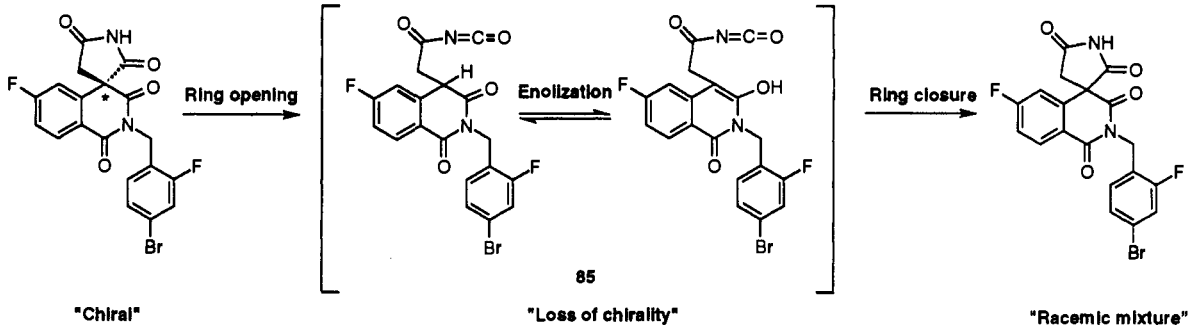

were removed in vacuo, and the acid chloride was dissolved in THF (20 mL). 4-Bromo-2-fluorobenzylamine (4.67 g, 22.91 mmol), triethylamine (15.96 mL, 114.55 mmol), and THF (150 mL) were placed into a second flask. The contents of the first flask were added into this second flask, and the mixture was stirred for 30 min. The suspension was poured into H_2O (1000 mL), stirred for 10 min, and acidified with HCl (2 N). The mixture was extracted with EtOAc, and the organic layer was dried over $MgSO_4$. Evaporation gave a yellowish solid which was recrystallized from acetone/ether/hexane (after cooling at −20 °C) to yield a white solid (**25**, 6.91 g, 86%): mp 149–150 °C; ^{1}H NMR (DMSO-d_6, 400 MHz) δ [3.67, 4.00 (s, 3H, CO_2CH_3 tautomeric)], [5.05 (q, J = 15.43 Hz, 5.4 (s), 2H, NCH_2), tautomeric], 5.03 (s, 1H, $CHCO_2CH_3$, tautomeric), 7.06–8.4 (m, 7H, Ar-*H*, tautomeric); IR (KBr, cm^{-1}) 1675 (CO), 1610 (CO); MS *m/e* 405 (M^+), 373 (M^+ − MeOH). Anal. ($C_{16}H_{13}BrFNO_4$) C, H, N.

Route c. 2-[(4-Bromo-2-fluorophenyl)methyl]-1,2,3,4-tetrahydro-4-(methoxycarbonyl)-1,3-dioxo-4-isoquinolineacetic acid 1,1-Dimethylethyl Ester (26a R^1 = H, R^2 = 4-Br-2-FC$_6$H$_3$CH$_2$, R^3 = CMe$_3$). *tert*-Butyl bromoacetate (2.81 mL, 17.37 mmol) was added to a suspension of 2-[(4-bromo-2-fluorophenyl)methyl]-1,2,3,4-tetrahydro-1,3-dioxo-4-isoquinolinecarboxylic acid methyl ester (**25**, R^1 = H, R^2 = 4-Br-2-FC$_6$H$_3$CH$_2$; 4.7 g, 11.58 mmol) and K_2CO_3 (3.19 g, 23.16 mmol) in DMF (100 mL). The mixture was stirred at 85 °C for 1 h, poured into H_2O (1000 mL), and extracted with EtOAc. The organic extracts were dried over $MgSO_4$. Evaporation and purification by flash chromatography (hexane/EtOAc, 4/1) gave a clear oil (**26a**, 5.69 g, 95%): ^{1}H NMR (DMSO-d_6, 400 MHz) δ 1.04 [s, 9H, $C(CH_3)_3$], 3.53 (s, 3H, CO_2CH_3), 3.60 [dd, J = 17.7 Hz, 2H, $CH_2CO_2C(CH_3)_3$], 5.14 (s, 2H, NCH_2), 7.17 (t, J = 8.25 Hz, 1H, Ar-*H*), 7.36 (dd, J = 8.36, 1.75 Hz, 1H, Ar-*H*), 7.6 (m, 3H, Ar-*H*), 7.77 (dt, J = 7.2, 1.27 Hz, 1H, Ar-*H*), 8.19 (dd, J = 8.25, 1.54 Hz, 1H, Ar-*H*); IR ($CHCl_3$, cm^{-1}) 1720 (CO), 1675 (CO); MS *m/e* 520 (M + H)$^+$, 464 (M^+ − $C(CH_3)_3$).

2-[(4-Bromo-2-fluorophenyl)methyl]-1,2,3,4-tetrahydro-4-(methoxycarbonyl)-1,3-dioxo-4-isoquinolineacetic Acid (26b, R^1 = H, R^2 = 4-Br-2-FC$_6$H$_3$CH$_2$, R^3 = OH). A mixture of 2-[(4-bromo-2-fluorophenyl)methyl]-1,2,3,4-tetrahydro-4-(methoxycarbonyl)-1,3-dioxo-4-isoquinolineacetic acid 1,1-dimethylethyl ester (**26a**, R^1 = H, R^2 = 4-Br-2-FC$_6$H$_3$CH$_2$, R^3 = CMe$_3$; 5.1 g, 9.8 mmol), CH_2Cl_2 (100 mL), and CF_3CO_2H (20 mL) was stirred at room temperature for 5 h. The volatiles were removed in vacuo, and the residue was purified on acid washed (5% H_3PO_4/MeOH) silica gel to give a white solid (**26b**, 4.12 g, 90%): mp 139–140 °C; ^{1}H NMR (DMSO-d_6, 400 MHz) δ 3.54 (s, 3H, CO_2CH_3), 3.66 (dd, J = 17.7 Hz, 2H, CH_2CO_2H), 5.13 (dd, J = 15.38 Hz, 2H, NCH_2), 7.14 (t, J = 8.24 Hz, 1H, Ar-*H*), 7.32 (dd, J = 8.3, 1.53 Hz, 1H, Ar-*H*), 7.54–7.63 (m, 3H, Ar-*H*), 7.74 (dt, J = 8.9, 1.26 Hz, 1H, Ar-*H*), 8.17 (dd, J = 7.8, 1.11 Hz, 1H, Ar-*H*), 12.65 (s, 1H, CO_2H); IR (KBr, cm^{-1}) 3300–2700 (CO_2H), 1740 (CO), 1715 (CO), 1670 (CO); MS *m/e* 464 (M + H)$^+$. Anal. ($C_{20}H_{15}BrFNO_6$) C, H, N.

4-(2-Amino-2-oxoethyl)-2-[(4-bromo-2-fluorophenyl)methyl]-1,2,3,4-tetrahydro-1,3-dioxo-4-isoquinolinecarboxylic Acid Methyl Ester (27, R^1 = H, R^2 = 4-Br-2-FC$_6$H$_3$CH$_2$). A mixture of 2-[(4-bromo-2-fluorophenyl)methyl]-1,2,3,4-tetrahydro-4-(methoxycarbonyl)-1,3-dioxo-4-isoquinolineacetic acid (**26b**, R^1 = H, R^2 = 4-Br-2-FC$_6$H$_3$CH$_2$, R^3 = OH; 4.0 g, 8.62 mmol) and $SOCl_2$ (20 g) was refluxed for 1 h. The volatiles were removed in vacuo, and the acid chloride was dissolved in THF (20 mL). The contents of this flask were added slowly to a second flask containing a freshly prepared saturated NH_3/THF solution (100 mL). After the addition, the mixture was stirred for 10 min, poured into H_2O (500 mL), acidified with HCl (2 N), and extracted with EtOAc. The organic extracts were dried over $MgSO_4$. Evaporation gave an off-white solid. The crude product was recrystallized from ether/hexane (after cooling to −20 °C) to yield a white solid (3.55 g, 89%): mp 180–181 °C; ^{1}H NMR (DMSO-d_6, 400 MHz) δ 3.53 (s, 3H, CO_2CH_3), 3.55 (dd, J = 16.6 Hz, 2H,

CH_2CONH_2), 5.12 (dd, J = 15.5 Hz, 2H, NCH_2), 6.88 (s, 1H, CONH), 7.23 (t, J = 8.25 Hz, 1H, Ar-H), 7.3 (dd, J = 8.36 Hz, 1.8 Hz, 1H, Ar-H), 7.45 (d, J = 7.9 Hz, 1H, Ar-H), 7.5–7.58 (m, 3H, Ar-H, CONH), 7.75 (dt, J = 7.63, 1.4 Hz, 1H, Ar-H), 8.13 (dd, J = 7.8, 1.17 Hz, 1H, Ar-H); IR (KBr, cm^{-1}) 3440 (NH), 1730 (CO), 1715 (CO); MS m/e 463 $(M+H)^+$. Anal. ($C_{20}H_{16}BrFN_2O_5$) C, H, N.

Route d. 2-[(4-Bromo-2-fluorophenyl)methyl]-4-(cyanomethyl)-1,2,3,4-tetrahydro-1,3-dioxo-4-isoquinolinecarboxylic Acid Methyl Ester (28, R^1 = H, R^2 = 4-Br-2-$FC_6H_3CH_2$). Freshly distilled $BrCH_2CN$ (1.3 mL, 18.21 mmol) was added to a cold (0 °C) suspension of 2-[(4-bromo-2-fluorophenyl)methyl]-1,2,3,4-tetrahydro-1,3-dioxo-4-isoquinolinecarboxylic acid methyl ester (25, R^1 = H, R^2 = 4-Br-2-$FC_6H_3CH_2$; 11.0 g, 25.9 mmol), K_2CO_3 (1.29 g, 9.35 mmol), DMF (30 mL), and acetone (30 mL). The mixture was stirred for 10 h at 0 °C and kept in the refrigerator for 4 days. The mixture was then poured into H_2O, acidified with HCl (2 N), and extracted with EtOAc. The organic extracts were dried over $MgSO_4$. Evaporation and purification by flash chromatography (hexane/EtOAc, 5/1) gave a white solid (3.95 g, 95%): mp 108–110 °C; ^1H NMR (DMSO-d_6, 400 MHz) δ 3.61 (s, 3H, CO_2CH_3), 3.72 (d, J = 17.0 Hz, 1H, HCHCN), 3.88 (d, J = 17.0 Hz, 1H, HCHCN), 5.14 (dd, J = 15.2 Hz, 2H, NCH_2), 7.17 (t, J = 8.3 Hz, 1H, Ar-H), 7.39 (dd, J = 8.3, 1.87 Hz, 1H, Ar-H), 7.55 (dd, J = 9.7, 2.1 Hz, 1H, Ar-H), 7.68 (m, 2H, Ar-H), 7.86 (dt, J = 7.7, 1.45 Hz, 1H, Ar-H), 8.21 (dd, J = 7.64, 1.25 Hz, 1H, Ar-H); IR (KBr, cm^{-1}) 2240 (CN), 1760 (CO), 1720 (CO), 1680 (CO); MS m/e 444 (M^+), 404 $(M^+ - CH_2CN)$. Anal. ($C_{20}H_{14}BrFN_2O_4$) C, H, N.

4-(2-Amino-2-oxoethyl)-2-[(4-bromo-2-fluorophenyl)methyl]-1,2,3,4-tetrahydro-1,3-dioxo-4-isoquinolinecarboxylic Acid Methyl Ester (27, R^1 = H, R^2 = 4-Br-2-$FC_6H_3CH_2$). Dry HCl gas was passed through a cold (0 °C) suspension of 2-[(4-bromo-2-fluorophenyl)methyl]-4-(cyanomethyl)-1,2,3,4-tetrahydro-1,3-dioxo-4-isoquinolinecarboxylic acid methyl ester (28, R^1 = H, R^2 = 4-Br-2-$FC_6H_3CH_2$; 3.8 g, 8.54 mmol) in dimethyl ether (100 mL) and anhydrous MeOH (1.03 mL, 25.62 mmol). During the introduction of the HCl gas the suspension turned into a solution. The mixture was kept at room temperature for 4.5 days, and then hexane (500 mL) was added. Most of the volatiles were removed in vacuo to the point that a white solid started to precipitate, and the mixture was cooled to 0 °C for 5 h. The precipitated solid was filtered, washed with hexane, and dried to yield a white solid (3.75 g, 95%): mp 180–181 °C. All spectroscopic data were identical to compound 27, prepared in route c. Anal. ($C_{20}H_{16}BrFN_2O_5$) C, H, N.

2-[(4-Bromo-2-fluorophenyl)methyl]spiro[isoquinoline-4(1H),3′-pyrrolidine]-1,2′,3,5′(2H)-tetrone (29, R^1 = H, R^2 = 4-Br-2-$FC_6H_3CH_2$; 40). Sodium hydride (80% dispersion in mineral oil, 0.25 g, 8.32 mmol) was added portionwise, over a 10-min period, to a solution of 4-(2-amino-2-oxoethyl)-2-[(4-bromo-2-fluorophenyl)methyl]-1,2,3,4-tetrahydro-1,3-dioxo-4-isoquinolinecarboxylic acid methyl ester (27, R^1 = H, R^2 = 4-Br-2-$FC_6H_3CH_2$; 3.5 g, 7.56 mmol) in DMF (20 mL). After being stirred for 20 min, the mixture was poured into H_2O, acidified with HCl (2 N), and extracted with EtOAc. The organic extracts were dried over $MgSO_4$. Evaporation and purification by flash chromatography on acid-washed (5% H_3PO_4 in MeOH) silica gel gave a white solid (2.58 g, 79%): mp 112–114 °C; ^1H NMR (DMSO-d_6, 400 MHz) δ (q, J = 18.24 Hz, 2H, CH_2CONH), 5.07 (s, 2H, NCH_2), 7.14 (t, J = 8.2 Hz, 1H, Ar-H), 7.33 (dd, J = 8.28, 1.71 Hz, 1H, Ar-H), 7.55 (dd, J = 9.8, 1.8 Hz, 1H, Ar-H), 7.62 (t, J = 7.6 Hz, 1H, Ar-H), 7.68 (d, J = 7.78 Hz, 1H, Ar-H), 7.78 (dt, J = 8.85 Hz, 1H, Ar-H), 8.15 (dd, J = 7.86, 1.3 Hz, 1H, Ar-H), 12.01 (s, 1H, CONHCO); IR (KBr, cm^{-1}) 3450 (NH), 3250 (NH), 1730 (CO), 1680 (CO); MS m/e 431 $(M+H)^+$. Anal. ($C_{13}H_{12}BrN_2O_4$) C, H, N.

2-Methylspiro[isoquinoline-4(1H),3′-pyrrolidine]-1,2′,3,5′-(2H)-tetrone (29, R^1 = H, R^2 = Me; 58). Lithium bis(trimethylsilyl)amide (17.24 mL, 17.24 mmol, 1.0 M in THF) was added over a 10-min period to a cold (−78 °C) solution of 4-(2-amino-2-oxoethyl)-1,2,3,4-tetrahydro-1,3-dioxo-4-isoquinolinecarboxylic acid methyl ester (27, R^1 = H, R^2 = Me; 2.5 g, 8.62 mmol) in anhydrous THF (80 mL). After being stirred at −78 °C for 10 h, the mixture was poured into H_2O, acidified with HCl (2 N), and extracted with EtOAc. The organic extracts were dried over $MgSO_4$. The crude product was purified by flash chromatography (hexane/EtOAc, 1/1) to yield a white solid (1.25 g, 56.8%): mp 224–225 °C; ^1H NMR (DMSO-d_6, 400 MHz) δ 3.23 (s, 3H, NCH_3), 3.43 (q, J = 18.3 Hz, 2H, CH_2CONCO), 7.60–7.62 (m, 2H, Ar-H), 7.74 (dt, J = 7.6, 1.22 Hz, 1H, Ar-H), 8.14 (dd, J = 7.72, 0.95 Hz, 1H, Ar-H), 12.0 (s, 1H, -CONHCO); IR (KBr, cm^{-1}) 3340 (NH), 1725 (CO), 1660 (CO); MS m/e 259 $(M+H)^+$. Anal. ($C_{13}H_{10}N_2O_4 \cdot {}^1/_4H_2O$) C, H, N.

6-Chloro-7-methoxy-2-methylspiro[isoquinoline-4(1H),3′-pyrrolidine]-1,2,3,5′(2H)-tetrone (29, R^1 represents 6-chloro-7-methoxy substitution, R^2 = Me; 68). In to a cold (−60 °C) solution of 4-(2-amino-2-oxoethyl)-6-chloro-7-methoxy-1,2,3,4-tetrahydro-1,3-dioxo-4-isoquinolinecarboxylic acid methyl ester (12.0 g, 33.85 mmol) in anhydrous DMF was added NaOMe (25% w/w in MeOH, 7.31 mL, 33.85 mmol) portionwise over a 10-min period. After being stirred for 5 min, the mixture was poured into 1 N HCl and extracted with EtOAc. The organic extracts were dried over $MgSO_4$. Evaporation and crystallization from acetone/ether gave a white solid (9.8 g, 90%): mp 259–261 °C; ^1H NMR (DMSO-d_6, 200 MHz) δ 3.23 (s, 3H, NCH_3), 3.35 (s, 2H, CH_2CO), 3.98 (s, 3H, OCH_3), 7.75 (s, 1H, Ar-H), 7.93 (s, 1H, Ar-H), 11.94 (s, 1H, CONHCO); IR (KBr, cm^{-1}) 3430 (NH), 1700 (CO), 1670 (CO); MS m/e 322 (M^+). Anal. ($C_{14}H_{11}ClN_2O_5$) C, H, N.

General Procedure for the Synthesis of Spiro[isoquinoline-4(1H),3′-pyrrolidine]-1,2′,3,5′(2H)-tetrones (33, Scheme 2). Compounds of the general structure **33** were synthesized from commercially available, appropriately substituted starting materials by the representative procedure illustrated for analog 78 (Table 2).

3-Methoxy-1-oxo-1H-2-benzopyran-4-carboxylic Acid Methyl Ester (30, R^1 = H). A mixture of 2-(2-carboxyphenyl)-propanedioic acid dimethyl ester (24, R^1 = H; 10.0 g, 39.68 mmol) and $SOCl_2$ (100 g) was refluxed for 2 h. The volatiles were removed in vacuo, and the crude product (acid chloride) was dissolved in THF (200 mL). Triethylamine (27.64 mL, 198.4 mmol) was added, and the mixture was stirred for 30 min. The yellowish suspension was poured into HCl (1 N, 1000 mL) and extracted with EtOAc. The organic extracts were dried over $MgSO_4$. Evaporation and crystallization from acetone/ether/hexane (after cooling to −20 °C) gave a white solid (87.6 g, 94.4%): mp 129–130 °C; ^1H NMR (DMSO-d_6, 400 MHz) δ 3.82 (s, 3H, CO_2Me), 4.03 (s, 3H, OMe), 7.42 (t, J = 7.26 Hz, 1H, Ar-H), 7.8 (t, J = 8.2 Hz, 1H, Ar-H), 7.9 (d, J = 8.3 Hz, 1H, Ar-H), 8.1 (d, J = 7.26 Hz, 1H, Ar-H); IR (KBr, cm^{-1}) 1740 (CO), 1685 (CO); MS m/e 234 (M^+), 206 $(M^+ - CO)$, 203 $(M^+ - OMe)$. Anal. ($C_{12}H_{10}O_5$) C, H.

2-(Cyanomethyl)-1,2,3,4-tetrahydro-1,3-dioxo-4-isoquinolinecarboxylic Acid Methyl Ester (31a, R^1 = H, R^2 = H). Aminoacetonitrile hydrochloride (6.32 g, 68.37 mmol) was added to a solution of 3-methoxy-1-oxo-1H-2-benzopyran-5-carboxylic acid methyl ester (30, R^1 = H; 8.09 g, 34.19 mmol) in DMF (100 mL). The suspension was stirred until all the materials had dissolved. Triethylamine (14.3 mL, 102.6 mmol) was added, and the mixture was stirred at 100 °C for 30 min, poured into H_2O, acidified with HCl (2 N), and extracted with EtOAc. The organic extracts were dried over $MgSO_4$. Evaporation and crystallization from acetone/ether/hexane (after cooling to −20 °C) gave a yellowish solid (6.5 g, 73.7%): mp 169–171 °C; ^1H NMR (DMSO-d_6, 400 MHz) δ (3.7, s, 3.98, s, 3H, CO_2CH_3, tautomeric), (4.92, s, 5.44, s, 2H, NCH_2CN, tautomeric), 7.2–8.4 (m, 4H, Ar-H, tautomeric); IR (KBr, cm^{-1}) 3400 (OH), 1670 (CO); MS m/e 258 (M^+), 226 $(M^+ - MeOH)$, 199 $(M^+ - CO_2Me)$. Anal. ($C_{13}H_{10}N_2O_4$) C, H, N.

2-(Cyanomethyl)-1,2,3,4-tetrahydro-4-(methoxycarbonyl)-1,3-dioxo-4-isoquinolineacetic acid 1,1-Dimethylethyl Ester (31b, R^1 = H, R^2 = $CH_2CO_2CMe_3$). *tert*-Butyl bromoacetate (6.1 mL, 37.8 mmol) was added to a suspension of 2-(cyanomethyl)-1,2,3,4-tetrahydro-1,3-dioxo-4-isoquinolinecarboxylic acid methyl ester (31a, R^1 = H, R^2 = H; 6.5 g, 25.19 mmol), K_2CO_3 (6.95 g, 50.38 mmol), and anhydrous DMF (100 mL). After being stirred at 85 °C for 3 h, the mixture was poured into H_2O, acidified with HCl (2 N), and extracted with EtOAc. The organic extracts were dried over $MgSO_4$. Evaporation and purification by flash chromatography on silica gel (hexane/EtOAc, 4/1) gave a white solid (8.5 g, 90.7%): mp 48–50 °C; ^1H NMR (DMSO-d_6, 200 MHz) δ 1.03 (s, 9H, CO_2CMe_3), 3.58 (s, 3H, CO_2CH_3), 3.64 (s, 2H,

CH_2CO_2), 5.05 (s, 2H, NCH_2CN), 7.64 (m, 2H, Ar-*H*), 7.78 (dd, *J* = 7.4, 2.0 Hz, 1H, Ar-*H*), 8.24 (dd, *J* = 8.2, 1.6 Hz, 1H, Ar-*H*); IR (KBr, cm^{-1}) 1745 (CO), 1730 (CO), 1670 (CO); MS *m/e* 373 ($M^+ + H$), 317 ($M^+ + H$, $-CMe_3$). Anal. ($C_{19}H_{20}N_2O_6$) C, H, N.

1,2,3,4-Tetrahydro-4-(methoxycarbonyl)-1,3-dioxo-2-[[5-(trifluoromethyl)-2-benzothiazolyl]methyl]-4-isoquinolineacetic Acid (32a, R^1 = H, R^3 = 5-CF_3, R^4 = OH). Triethylamine (3.65 mL) was added to a mixture of 3-amino-4-mercaptobenzotrifluoride hydrochloride (6.1 g, 26.2 mmol) and EtOH (150 mL). After the mixture was stirred for 10 min, 2-(cyanomethyl)-1,2,3,4-tetrahydro-4-(methoxycarbonyl)-1,3-dioxo-4-isoquinolineacetic acid 1,1-dimethylethyl ester (**31b**, R^1 = H, R^2 = $CH_2CO_2CMe_3$; 6.5 g, 17.47 mmol) was added, and the mixture was refluxed for 15 h, poured into H_2O, acidified with HCl (2 N), and extracted with EtOAc. The organic extracts were dried over $MgSO_4$. Evaporation gave an oil (9.6 g) which was dissolved in CH_2Cl_2 (80 mL). Trifluoroacetic acid (20 mL) was added, and the mixture was stirred at room temperature for 8 h. The volatiles were removed in vacuo, and the residue was purified by flash chromatography on acid-washed (5% H_3PO_4 in MeOH) silica gel to give a white solid (6.3 g, 73.3%): mp 199–201 °C; ^1H NMR (DMSO-d_6, 400 MHz) δ 3.57 (s, 3H, CO_2CH_3), 3.68 (dd, *J* = 17.85 Hz, 2H, CH_2CO_2H), 5.61 (s, 2H, NCH_2), 7.62 (m, 2H, Ar-*H*), 7.81 (m, 2H, Ar-*H*), 8.2 (dd, *J* = 7.9, 1.04 Hz, 1H, Ar-*H*), 8.33 (dd, *J* = 8.5, 0.92 Hz, 1H, Ar-*H*), 8.34 (d, *J* = 0.83 Hz, 1H, Ar-*H*); IR (KBr, cm^{-1}) 3200–2500 (CO_2H), 1750 (CO), 1710 (CO), 1670 (CO); MS *m/e* 492 (M^+), 448 ($M^+ - CO_2$), 416 ($M^+ - CO_2$ – MeOH). Anal. ($C_{22}H_{15}F_3N_2O_6S$) C, H, N.

4-(2-Amino-2-oxoethyl)-1,2,3,4-tetrahydro-1,3-dioxo-2-[[5-(trifluoromethyl)-2-benzothiazolyl]methyl]-4-isoquinolinecarboxylic Acid Methyl Ester (32b, R^1 = H, R^3 = 5-CF_3, R^4 = NH_2). A mixture of 1,2,3,4-tetrahydro-4-(methoxycarbonyl)-1,3-dioxo-2-[[5-(trifluoromethyl)-2-benzothiazolyl]methyl]-4-isoquinolineacetic acid (**32a**, R^1 = H, R^3 = 5-CF_3, R^4 = OH; 2.5 g, 5.08 mmol) and $SOCl_2$ (25 g) was refluxed for 1 h. The volatiles were removed in vacuo, and the product (acid chloride) was taken in THF (20 mL) and added to a freshly prepared, saturated NH_3/THF solution (20 mL). After being stirred for 10 min, the mixture was poured into HCl (1 N, 500 mL) and extracted with EtOAc. The organic extracts were dried over $MgSO_4$. Evaporation and purification by flash chromatography on silica gel (hexane/EtOAc, 1/1) gave a light yellow solid (2.1 g, 84%): mp 198–200 °C; ^1H NMR (DMSO-d_6, 400 MHz) δ 3.53 (dd, *J* = 16.6 Hz, 2H, CH_2CONH_2), 3.56 (s, 3H, CO_2CH_3), 5.53 (d, *J* = 15.77 Hz, 1H, NHCH), 5.6 (d, *J* = 15.77 Hz, 1H, NHCH), 6.84 (br s, 1H, CONH), 7.49 (m, 2H, Ar-H, CONH), 7.6 (t, *J* = 7.47 Hz, 1H, Ar-*H*), 7.68 (m, 2H, Ar-*H*), 8.17 (dd, *J* = 7.9, 1.45 Hz, 1H, Ar-*H*), 8.34 (m, 2H, Ar-*H*); IR (KBr, cm^{-1}) 3420 (NH), 3180 (NH), 1745 (CO), 1710 (CO), 1660 (CO); MS *m/e* 491 (10, M^+). Anal. ($C_{22}H_{16}F_3N_3O_5S$) C, H, N.

2-[[5-(Trifluoromethyl)-2-benzothiazolyl]methyl]spiro[isoquinoline-4(1*H*),3′-pyrrolidine]-1,2′,3,6′(2*H*)-tetrone (33, R^1 = H, R^3 = 5-CF_3). Sodium hydride (80% dispersion in oil, 0.11g, 3.25 mmol) was added portionwise, over a 5-min period, to a mixture of 4-[(aminocarbonyl)methyl]-1,2,3,4-tetrahydro-1,3-dioxo-2-[[5-(trifluoromethyl)-2-benzothiazolyl]methyl]-4-isoquinolineacetic acid methyl ester (**32b**, R^1 = H, R^3 = 5-CF_3, R^4 = NH_2; 1.6 g, 3.34 mmol) and anhydrous DMF (20 mL). After being stirred for 30 min the mixture was poured into H_2O (1000 mL), acidified with HCl (2 N), and extracted with EtOAc. The organic extracts were dried over $MgSO_4$. Evaporation and purification by flash chromatography on silica gel (hexane/EtOAc, 1/2) gave a white solid (1.2 g, 80.3%): mp 122–124 °C; ^1H NMR (DMSO-d_6, 400 MHz) δ 3.44 (dd, *J* = 18.26 Hz, 2H, CH_2CO), 5.56 (s, 2H, NCH_2), 7.66 (dt, *J* = 7.26, 1.04 Hz, 1H, Ar-*H*), 7.75 (m, 2H, Ar-*H*), 7.82 (dt, *J* = 7.88, 1.66 Hz, 1H, Ar-*H*), 8.22 (dd, *J* = 7.88, 1.45 Hz, 1H, Ar-*H*), 8.33 (m, 2H, Ar-*H*), 12.05 (s, 1H, CONHCO); IR (KBr, cm^{-1}) 3400 (NH), 3240 (NH), 1725 (CO), 1680 (CO); MS *m/e* 459 (82, M^+). Anal. ($C_{21}H_{12}F_3N_3O_4S$) C, H, N.

Preparation of the Enantiomers. Enantiomers 81-84 (Table 7) were synthesized from the appropriately substituted homophthalic anhydrides (Scheme 3) by the representative procedures illustrated for the analogs 81 and 82.

2-[(4-Bromo-2-fluorophenyl)methyl]-1,3(2*H*,3*H*)-isoquinolinedione (34, R^1 = H). 4-Bromo-2-fluorobenzylamine hydrochloride (22.0 g, 91.5 mmol) and triethylamine (12.75 mL, 91.5 mmol) were added to a suspension of homophthalic anhydride (14.8 g, 91.36 mmol) in THF (200 mL). The mixture was stirred at room temperature for 1 h, and the volatiles were removed in vacuo. The residue was taken in DMF (150 mL) and refluxed for 15 h. After being cooled to room temperature, the brownish solution was poured into H_2O, extracted with EtOAc, and dried over $MgSO_4$. Evaporation and purification by flash chromatography (hexane/EtOAc, 2/1) gave a white solid (16.1 g, 51%): mp 128–129 °C; ^1H NMR (DMSO-d_6, 200 MHz) δ 4.24 (s, 2H, CH_2CON), 5.04 (s, 2H, NCH_2), 7.23 (t, *J* = 7.8 Hz, 1H, Ar-*H*), 7.3 (d, *J* = 7.65 Hz, 1H, Ar-*H*), 7.4–7.56 (m, 3H, Ar-*H*), 7.65 (t, *J* = 7.6 Hz, Ar-*H*), 8.06 (d, *J* = 7.8 Hz, 1H, Ar-*H*); IR (KBr, cm^{-1}) 1675 (CO); M/S *m/e* 347 (M^+). Anal. ($C_{16}H_{11}BrFNO_2$) C, H, N.

2-[(4-Bromo-2-fluorophenyl)methyl]-1,2,3,4-tetrahydro-1,3-dioxo-4-isoquinolinecarboxylic Acid Methyl Ester (35a, R^1 = H, R^2 = H). Lithium bis(trimethylsilyl)amide (1.0 M solution in THF, 56.91 mL, 56.91 mmol) was added dropwise over a 10-min period to a cold (−78 °C) solution of 2-[(4-bromo-2-fluorophenyl)methyl]-1,3(2*H*,3*H*)-isoquinolinedione (**34**, R^1 = H; 9.0 g, 25.86 mmol) in anhydrous THF (120 mL). After the mixture was stirred for 3 h, (−)-menthyl chloroformate (8.48 mL, 38.79 mmol) was added, and the reaction mixture was allowed to warm up to room temperature. The mixture turned dark during that period. It was stirred for 30 min and quenched with aqueous NH_4Cl. The dark solution was poured into H_2O, acidified with HCl (2 N), and extracted with EtOAc. The organic extracts were dried over $MgSO_4$. Evaporation and purification by flash chromatography on acid-washed (5% H_3PO_4 in MeOH) silica gel gave a clear oil (10.2 g, 74%): ^1H NMR (DMSO-d_6, 200 MHz) δ 0.3–1.9 (m, 18H, *menthyl*), 4.3–4.6 (m, 1H, CO_2CH), 5.0–5.35 (m, 2H, NCH_2), 7.1–7.8 (m, 6H, Ar-*H*), 8.2–8.5 (m, 1H, Ar-*H*); M/S *m/e* 529 (M^+), 391 (M^+ menthyl); IR (KBr, cm^{-1}) 1780 (CO), 1740 (CO), 1690 (CO).

2-[(4-Bromo-2-fluorophenyl)methyl]-1,2,3,4-tetrahydro-4-(menthoxycarbonyl)-1,3-dioxo-4-isoquinolineacetic Acid 1,1-Dimethylethyl Ester (35b, R^1 = H, R^2 = $CH_2CO_2CMe_3$). *tert*-Butyl bromoacetate (4.64 mL, 28.74 mmol) was added to a mixture of 2-[(4-bromo-2-fluorophenyl)methyl]-1,2,3,4-tetrahydro-1,3-dioxo-4-isoquinolinecarboxylic acid menthyl ester (**35a**, R^1 = H, R^2 = H; 7.62 g, 14.37 mmol) and K_2CO_3 (3.86 g, 28.74 mmol) in DMF (100 mL). The mixture was stirred at 85 °C for 2 h, poured into H_2O (1000 mL), and extracted with EtOAc. The organic extracts were dried over $MgSO_4$. Evaporation and purification by flash chromatography (hexane/EtOAc, 4/1) gave a clear oil (6.9 g, 74% yield, diastereomeric mixture). The two diastereomers were separated by preparative HPLC on preparative Pac silica column (m pora Si/125Å, 15–20 m silica 30 cm × 2 in.), using an elution with hexane/CH_2Cl_2 to give the less polar diastereomer as a white solid (**36a**, 2.4 g) and the more polar diastereomer as a clear oil (**37a**, 2.2 g). The diastereomeric purity was determined by analytical HPLC on Dynamax silica 25 cm × 4.1 mm and was found to be greater than 99% for both diastereomers. **Spectroscopic data for less polar diastereomer 36a:** mp 50-51 °C; ^1H NMR (DMSO-d_6, 400 MHz) δ 0.42 (m, 1H, *menthyl*), 0.56 (d, *J* = 7.4 Hz, 3H, $CHCH_3$), 0.64 (d, *J* = 7.4 Hz, 3H, $CHCH_3$), 0.72 (d, *J* = 6.2 Hz, 3H, $CHCH_3$), 0.92–0.97 (m, 2H, *menthyl*), 1.05 [s, 9H, $(CH_3)_3$], 1.22–1.39 (m, 3H, *menthyl*), 2.5–2.6 (m, 2H, *menthyl*), 3.55 (dd, *J* = 17.02 Hz, 2H, CH_2CO_2), 4.46 (m, 1H, OCH), 5.10 (dd, *J* = 15.02 Hz, 2H, NCH_2), 7.2 (t, *J* = 8.16 Hz, 1H, Ar-*H*), 7.33 (dd, *J* = 8.44, 1.7 Hz, 1H, Ar-*H*), 7.53 (dd, *J* = 9.7, 1.85 Hz, 1H, Ar-*H*), 7.6–7.77 (m, 2H, Ar-*H*), 7.79 (dt, *J* = 7.67, 1.35 Hz, 1H, Ar-*H*), 8.2 (dd, *J* = 7.77, 1.0 Hz, 1H, Ar-*H*); IR (KBr, cm^{-1}) 1715 (CO), 1670 (CO); M/S *m/e* 655 (M + H)$^+$, 587 [M + H − $C(CH_3)_3$]$^+$. **Spectroscopic data for more polar diastereomer 37a:** ^1H NMR (DMSO-d_6, 400 MHz) δ 0.1 (d, *J* = 6.6 Hz, 3H, $CHCH_3$), 0.15 (m, 1H, *menthyl*), 0.42 (d, *J* = 6.6 Hz, 3H, $CHCH_3$), 0.58–0.61 (m, 1H, *menthyl*), 0.64–0.9 (m, 3H, *menthyl*), 0.78 (d, *J* = 6.2 Hz, 3H, $CHCH_3$), 1.04 [s, 9H, $C(CH_3)_3$], 1.2–1.38 (m, 1H, *menthyl*), 1.4 (m, 1H, *menthyl*), 1.43–1.47 (m, 2H, *menthyl*), 3.54 (dd, *J* = 17.0 Hz, 2H, CH_2CO_2), 4.24 (m, 1H, OCH), 4.96 (d, *J* = 14.56 Hz, 1H, NCH), 5.32 (d, *J* = 14.56 Hz, 1H, NCH), 7.29 (t, *J* = 7.96 Hz, 1H, Ar-*H*), 7.35 (dd, *J* = 8.31, 1.8 Hz, 1H, Ar-*H*), 7.53–7.55 (m, 2H, Ar-*H*), 7.61 (dt, *J* = 8.29, 0.9 Hz, 1H, Ar-*H*), 7.76 (dt, *J* = 7.65, 1.4 Hz, 1H, Ar-*H*), 8.22 (dd, *J* = 7.85, 1.2 Hz, 1H, Ar-*H*); IR ($CHCl_3$, cm^{-1}) 1715

(CO), 1670 (CO); M/S *m/e* 643 (M^+), 587 [$M^+ + H - C(CH_3)_3$], 4.49 [$M^+ + H - C(CH_3)_3$ – menthyl].

2-[(4-Bromo-2-fluorophenyl)methyl]-1,2,3,4-tetrahydro-4-(menthoxycarbonyl)-1,3-dioxo-4-isoquinolineacetic Acid (36b, R^1 = H, R^3 = OH). A mixture of 2-[(4-bromo-2-fluorophenyl)methyl]-1,2,3,4-tetrahydro-4-(menthoxycarbonyl)-1,3-dioxo-4-isoquinolineacetic acid 1,1-dimethylethyl ester (**36a**, R^1 = H, R^3 = $OCMe_3$; 7.0 g, 10.87 mmol), CH_2Cl_2 (60 mL), and CF_3CO_2H (15 mL) was stirred at room temperature for 5 h. The volatiles were removed in vacuo, and the residue was purified by flash chromatography, on acid washed (5% H_3PO_4 in MeOH) silica gel, to give a white solid (6.0 g, 94%): mp 79–80 °C; ^{1}H NMR (DMSO-d_6, 400 MHz) δ 0.5 (q, *J* = 7.4 Hz, 1H, C*H*CH_3), 0.66 (d, *J* = 6.6 Hz, 3H, CHC*H*$_3$), 0.71 (d, *J* = 7.4 Hz, 3H, CHC*H*$_3$), 0.82–1.05 (m, 3H, *menthyl*), 1.2–1.56 (m, 5H, *menthyl*), 3.6 (dd, *J* = 17.65 Hz, 2H, C*H*$_2CO_2H$), 4.46 (dt, *J* = 10.67, 3.9 Hz, 1H, OC*H*), 5.1 (dd, *J* = 15.2 Hz, 2H, NC*H*$_2$), 7.17 (t, *J* = 8.2 Hz, 1H, Ar-*H*), 7.3 (dd, *J* = *J* = 8.28, 1.7 Hz, 1H, Ar-*H*), 7.53 (dd, *J* = 9.8, 1.9 Hz, 1H, Ar-*H*), 7.6 (m, 2H, Ar-*H*), 7.77 (dt, *J* = 7.64, 1.4 Hz, 1H, Ar-*H*), 8.17 (dd, *J* = 8.16, 1.5 Hz, 1H, Ar-*H*); IR (KBr, cm^{-1}) 3350–2700 (CO_2H), 1745 (CO), 1720 (CO), 1675 (CO); M/S *m/e* 587 (M^+), 449 (M^+ – menthyl]. Anal. ($C_{29}H_{31}BrFNO_6$) C, H, N.

2-[(4-Bromo-2-fluorophenyl)methyl]-1,2,3,4-tetrahydro-4-(methoxycarbonyl)-1,3-dioxo-4-isoquinolineacetic Acid (37b, R^1 = H, R^3 = OH). A mixture of 2-[(4-bromo-2-fluorophenyl)methyl]-1,2,3,4-tetrahydro-4-(menthoxycarbonyl)-1,3-dioxo-4-isoquinolineacetic acid 1,1-dimethylethyl ester (**37a**, R^1 = H, R^3 = $OCMe_3$; 6.8 g, 10.56 mmol), CH_2Cl_2 (80 mL), and CF_2CO_2H (20 mL) was stirred at room temperature for 5 h. The volatiles were removed in vacuo, and the residue was purified by flash chromatography on acid-washed (5% H_3PO_4 in MeOH) silica gel to give a white solid (5.81 g, 94%): mp 131–132 °C; ^{1}H NMR (DMSO-d_6, 400 MHz) δ 0.16 (d, *J* = 6.6 Hz, 3H, CHC*H*$_3$), 0.22 (q, *J* = 7.2 Hz, 3H, C*H*CH_3), 0.42 (d, *J* = 6.6 Hz, 3H, CHC*H*$_3$), 0.6 (m, 1H, *menthyl*), 0.8 (d, *J* = 7.2 Hz, 3H, CHC*H*$_3$), 0.7–0.95 (m, 4H, *menthyl*), 1.25 (m, 1H, *menthyl*), 1.42 (m, 1H, Ar-*H*), 1.45–1.48 (m, 2H, *menthyl*), 3.6 (dd, *J* = 17.75 Hz, 2H, C*H*$_2$-CO_2H), 4.25 (dt, *J* = 10.7, 3.2 Hz, 1H, OC*H*), 5.0 (dd, *J* = 14.7 Hz, 2H, NC*H*$_2$), 7.27 (t, *J* = 8.05 Hz, 1H, Ar-*H*), 7.34 (dd, *J* = 8.28, 1.7 Hz, 1H, Ar-*H*), 7.53–7.61 (m, 3H, Ar-*H*), 7.74 (dt, *J* = 7.65, 1.3 Hz, 1H, Ar-*H*), 8.2 (dd, *J* = 7.86, 1.16 Hz, 1H, Ar-*H*); IR (KBr, cm^{-1}) 3550–2700 (CO_2H), 1745 (CO), 1720 (CO), 1675 (CO); M/S *m/e* 588 (M + H)$^+$, 450 (M + H – menthyl). Anal. ($C_{29}H_{31}BrFNO_6$), C, H, N.

4-(2-Amino-2-oxoethyl)-2-[(4-bromo-2-fluorophenyl)-methyl]-1,2,3,4-tetrahydro-1,3-dioxo-4-isoquinolinecarboxylic Acid Menthyl Ester (36c, R^1 = H, R^3 = NH_2). A mixture of 2-[(4-bromo-2-fluorophenyl)methyl]-1,2,3,4-tetrahydro-4-(menthoxycarbonyl)-1,3-dioxo-4-isoquinolineacetic acid (**36b**, R^1 = H, R^3 = OH; 5.5 g, 9.35 mmol) and $SOCl_2$ (30 mL) was refluxed for 2 h. The volatiles were removed in vacuo, and the product (acid chloride) was dissolved in THF (20 mL). The contents of the first flask were added slowly to a second flask containing a freshly prepared, saturated NH_3/THF solution (100 mL). After the addition the mixture was stirred for 15 min, poured into H_2O (500 mL), acidified with HCl (2 N), and extracted with EtOAc. The organic extracts were dried over $MgSO_4$. Evaporation and purification by flash chromatography (hexane/EtOAc, 1/1) gave a white solid (4.86 g, 88%): mp 84–85 °C; ^{1}H NMR (DMSO-d_6, 400 MHz) δ 0.44 (q, *J* = 7.4 Hz, 1H, CHC*H*$_3$), 0.57 (d, *J* = 6.6 Hz, 3H, CHC*H*$_3$), 0.64 (d, *J* = 6.6 Hz, 3H, CHC*H*$_3$), 0.71 (d, *J* = 7.4 Hz, 3H, CHC*H*$_3$), 0.84–1.04 (m, 3H, *menthyl*), 1.2–1.4 (m, 2H, *menthyl*), 1.42–1.58 (m, 3H, *menthyl*), 3.47 (dd, *J* = 16.57 Hz, 2H, C*H*$_2$CONH$_2$), 4.46 (dt, *J* = 10.7 Hz, 1H, OC*H*), 5.05 (dd, *J* = 15.4 Hz, 2H, NC*H*$_2$), 6.87 (s, 1H, CONH), 7.27 (m, 2H, Ar-*H*), 7.43 (d, *J* = 7.8 Hz, 1H, Ar-*H*), 7.55 (m, 3H, Ar-*H*, CONH), 7.26 (dt, *J* = 7.6, 1.1 Hz, 1H, Ar-*H*), 8.13 (dd, *J* = 7.85, 1.1 Hz, 1H, Ar-*H*); IR (KBr, cm^{-1}) 3450 (NH), 3320 (NH), 1730 (CO), 1715 (CO), 1670 (CO); M/S *m/e* 587 (M + H)$^+$, 449 (M + H – menthyl). Anal. ($C_{29}H_{32}BrFN_2O_5$) C, H, N.

4-(2-Amino-2-oxoethyl)-2-[(4-bromo-2-fluorophenyl)-methyl]-1,2,3,4-tetrahydro-1,3-dioxo-4-isoquinolinecarboxylic Acid Menthyl Ester (37c, R^1 = H, R^3 = NH_2). A mixture 2-[(4-bromo-2-fluorophenyl)methyl]-1,2,3,4-tetrahydro-4-(menthoxycarbonyl)-1,3-dioxo-4-isoquinolineacetic acid (**37b**, R^1 = H, R^3 = OH; 5.5 g, 9.35 mmol) and $SOCl_2$ (30 mL) was refluxed for 2 h. The volatiles were removed in vacuo, and the residue was dissolved in THF (20 mL). The contents of the first flask were added slowly to a second flask containing a freshly prepared, saturated NH_3/THF solution (100 mL). After the addition the mixture was stirred for 15 min, poured into H_2O (500 mL), acidified with HCl (2 N), and extracted with EtOAc. The organic extracts were dried over $MgSO_4$. Evaporation and purification by flash chromatography (hexane/EtOAc, 1/1) gave a white solid (4.75 g, 86%); mp 151–152 °C; ^{1}H NMR (DMSO-d_6, 200 MHz) δ 0.14 (d, *J* = 6.6 Hz, 3H, CHC*H*$_3$), 0.25 (m, 1H, *menthyl*), 0.4 (d, *J* = 6.8 Hz, 3H, CHC*H*$_3$), 0.6 (m, 3H, *menthyl*), 0.77 (d, *J* = 7.0 Hz, 3H, CHC*H*$_3$), 1.3–1.6 (m, 5H, *menthyl*), 3.49 (dd, *J* = 16.6 Hz, 2H, C*H*$_2$CONH$_2$), 4.3 (dt, *J* = 10.6, 3.8 Hz, 1H, OC*H*), 4.9 (d, *J* = 14.6 Hz, 1H, NC*H*), 5.26 (dd, *J* = 14.6 Hz, 1H, NC*H*), 5.26 (d, *J* =14.6 Hz, 1H, NC*H*), 6.85 (s, 1H, CONH), 7.31 (m, 2H, Ar-*H*), 7.4 (d, *J* = 7.4 Hz, 1H, Ar-*H*), 7.5–7.6 (m, 3H, Ar-*H*, CONH), 7.7 (dt, *J* = 7.4, 2.0 Hz, 1H, Ar-*H*), 8.14 (dd, *J* = 7.4, 1.6 Hz, 1H, Ar-*H*); IR (KBr, cm^{-1}) 3460 (NH), 3314 (NH), 1715 (CO), 1675 (CO); M/S *m/e* 587 (M + H)$^+$, 449 (M + H – menthyl). Anal. ($C_{29}H_{32}BrFN_2O_5$) C, H, N.

(*S*)-(–)-2-[(4-Bromo-2-fluorophenyl)methyl]spiro[isoquinoline-4(1*H*),3′-pyrrolidine]-1,2′,3,5′(2*H*)-tetrone (38, R^1 = H; 81). Lithium bis(trimethylsilyl)amide (1.0 M in THF, 5.96 mL, 5.96 mmol) was added dropwise over a 5-min period to a cold (–78 °C) solution of 4-(2-amino-2-oxoethyl)-2-[(4-bromo-2-fluorophenyl)methyl]-1,2,3,4-tetrahydro-1,3-dioxo-4-isoquinolinecarboxylic acid menthyl ester (**37c**, R^1 = H, R^3 = NH_2; 3.5 g, 5.96 mmol) in anhydrous THF (80 mL). After being stirred at –78 °C for 20 min the reaction was quenched with HCl (2 N) and the mixture was poured into H_2O and extracted with EtOAc. The organic extracts were dried over $MgSO_4$. Evaporation and purification by flash chromatography on acid washed (5% H_3PO_4 in MeOH) silica gel, eluting solvent hexane/EtOAc, 2/1, gave a white solid, which was recrystallized once from diethyl ether (after cooling to –20 °C) to yield a crystalline white solid (1.1 g, 43%). The enantiomeric purity was determined by analytical HPLC (Chiralcel OB, 2.5 cm × 0.46, mobile phase, 1/1 hexane/EtOAc) and was found to be 99.6% ee. The absolute stereochemistry of this enantiomer has been determined as being *S* from the X-ray crystallographic analysis: mp 170–175 °C; ^{1}H NMR (DMSO-d_6, 400 MHz) δ 3.4 (dd, *J* = 18.35 Hz, 2H, C*H*$_2$-CONH), 5.06 (s, 2H, NC*H*$_2$), 7.14 (t, *J* = 8.21 Hz, 1H, Ar-*H*), 7.32 (dd, *J* = 8.34, 1.67 Hz, 1H, Ar-*H*), 7.53 (dd, *J* = 9.83, 1.87 Hz, 1H, Ar-*H*), 7.6 (dt, *J* = 7.85, 1.03 Hz, 1H, Ar-*H*), 7.68 (d, *J* = 7.76 Hz, 1H, Ar-*H*), 7.77 (dt, *J* = 7.53, 1.34 Hz, 1H, Ar-*H*), 8.15 (dd, *J* = 7.88, 1.25 Hz, 1H, Ar-*H*), 12.01 (s, 1H, CONHCO); IR (KBr, cm^{-1}) 3340 (NH), 1735 (CO), 1710 (CO), 1765 (CO); M/S *m/e* 430 (M^+), 387 (M^+ – CONH); $[\alpha]^{25}_D$ = –63.3 (*c* = 1.02, EtOAc). Anal. ($C_{16}H_{12}BrFN_2O_4$) C, H, N.

(*R*)-(+)-2-[(4-Bromo-2-fluorophenyl)methyl]spiro[isoquinoline-4(1*H*)-3′-pyrrolidine]-1,2′,3,5′(2*H*)-tetrone (39, R^1 = H; 82). Lithium bis(trimethylsilyl)amide (1.0 M in THF, 5.11 mL, 5.11 mmol) was added dropwise over a 5-min period to a cold (–78 °C) solution of 4-(2-amino-2-oxoethyl)-2-[(4-bromo-2-fluorophenyl)methyl)]-1,2,3,4-tetrahydro-1,3-dioxo-4-isoquinolinecarboxylic acid menthyl ester (**37c**, R^1 = H, R^3 = NH_2; 3.0 g, 5.11 mmol) in anhydrous THF (60 mL). After being stirred at –78 °C for 20 min the reaction was quenched with HCl (2 N), and the mixture was poured into H_2O and extracted with EtOAc. The organic extracts were dried over $MgSO_4$. Evaporation and purification by flash chromatography on acid washed (5% H_3PO_4 in MeOH) silica gel, eluting solvent hexane/EtOAc, 2/1, gave a white solid, which was recrystallized once from ethyl ether (at –20 °C) to yield a crystalline white solid (1.2 g, 43%). The enantiomeric purity was determined by analytical HPLC (Chiralcel OB, 25 cm × 0.46, mobile phase, 1/1 hexane/EtOAc) and was found to be 99.2% ee: mp 175–176 °C; ^{1}H NMR (DMSO-d_6, 400 MHz) δ 3.4 (dd, *J* = 18.35 Hz, 2H, C*H*$_2$CONH), 5.06 (s, 2H, NC*H*$_2$), 7.14 (t, *J* = 8.21 Hz, 1H, Ar-*H*), 7.32 (dd, *J* = 8.34, 1.67 Hz, 2H, Ar-*H*), 7.53 (dd, *J* = 9.83, 1.87 Hz, 1H, Ar-*H*), 7.6 (dt, *J* = 7.85, 1.03 Hz, 1H, Ar-*H*), 7.68 (d, *J* = 7.76 Hz, 1H, Ar-*H*), 7.77 (dt, *J* = 7.53, 1.34 Hz, 1H, Ar-*H*), 8.15 (dd, *J* = 7.88, 1.25 Hz, 1H, Ar-*H*), 12.01 (s, 1H, CONHCO); IR (KBr, cm^{-1}) 3340 (NH), 1735 (CO), 1710 (CO), 1765 (CO); M/S *m/e* 430 (M^+), 387 (M^+ – CONH); $[\alpha]^{25}_D$ = +62.3 (*c* = 0.8, EtOAc). Anal. ($C_{19}H_{12}BrFN_2O_4$) C, H, N.

Single-Crystal X-ray Analyses. (a) Enantiomer 81. Suitable crystals of (−)-81 were grown from ethyl ether. The compound crystallized in the orthorhombic space group $P2_12_12_1$ with unit cell dimensions a = 6.3737(13) Å, b = 13.736(2) Å, c = 19.246(2) Å; V = 1684(4) Å^3; Z = 4; ρ(calcd) = 1.70 g cm^{-3}; F(000) = 864; T = 234 K; λ(Cu Kα) = 1.541 78 Å; crystal size (mm) 0.35 × 0.42 × 0.50; $C_{19}H_{12}BrFN_2O_4$; M = 431.2.

A Nicolet R3M automated diffractometer was used to collect the crystallographic data. The standard reflections used to monitor data collection did not show significant deviations within the period of data collection. Unit cell constants were determined by a least-squares fit of the 2q values of 20 reflections having 45° ≤ 2θ ≤ 50°. The space group determination was assigned by observation of the following systematic extinction's: $h00, h = 2n + 1, 0k0, k = 2n + 1, 00l, l = 2n + l$. Raw intensities were reduced to structure factor amplitudes by correction for scan speed, background, Lorentz, and polarization effects. Empirical absorption corrections were applied based on the azimuthal scans of 10 reflections representing the range of 20 values. The structure was solved by direct methods and refined using the Nicolet SHELXTL V (Micro Eclipse) programs. During the final stages of refinement, all non-hydrogen atoms were refined with anisotropic temperature factors, all C-H hydrogens were included at idealized positions [C–H 0.96 Å, X–C–H 109° or 120°, B(H) = 1.2B(C)], and the N-H hydrogen was located on a difference Fourier map and fixed at the observed position. An n refinement was carried out to determine the absolute configuration. The value for n refined to 1.04 (5) for the structure with C(4) (*S*) stereochemistry indicating that to be the correct absolute stereochemistry.[53] The analytical scattering factors for the neutral atoms were used,[54] and all non-hydrogen scattering factors were corrected for both the real and imaginary components of anomalous dispersion.[54]

There is one short intermolecular interaction, that being a hydrogen bond between N(12) and O(22) with distances and angles as follows: N(12)–O(22), 2.94 Å; H(12)–O(22), 1.79 Å; N(12)–H(12)–O(22), 155°. The final R index for (−)-81 was 0.053.

(b) Enantiomer (+)-83. Suitable crystals of (+)-83 were grown from acetone/ethyl ether. The compound crystallized in the orthorhombic space group $P2_12_12_1$ with unit cell dimensions a = 6.4430(6) Å, b = 13.6414(12) Å, c = 19.389(2) Å; V = 1704.1(3) Å^3; Z = 4; ρ(calcd) = 1.751 mg cm^{-1}; F(000) = 896; T = 296 K; λ(Cu Kα) = 1.541 78 Å; crystal size (mm) = 0.10 × 0.30 × 0.42; $C_{19}H_{11}BrF_2N_2O_4$; M = 449.2.

A Siemens R3M automated diffractometer was used to collect the crystallographic data. The standard reflections used to monitor data collection did not show significant deviations within the period of data collection. Unit cell constants were determined by a least-squares fit of the 2q values of 25 reflections having 45° ≤ 2θ ≤ 50°. Raw intensities were reduced to structure factor amplitudes by correction for scan speed, background, Lorentz, and polarization effects. The structure was solved by direct methods and refined using the Siemens SHELXTL Plus (VMS) package of programs. Hydrogen atoms were located on a difference fourier map and were subsequently entered at idealized positions. An n refinement to determine the absolute configuration gave indefinite results (n = 0.10 + 0.06). The analytical scattering factors for the neutral atoms were used,[53] and all non-hydrogen scattering factors were corrected for both the real and imaginary components of anomalous dispersion.[54] The largest residual peaks were in the vicinity of the bromine atom. There is one intermolecular hydrogen bond formed between N(12) and O(22) with distances and angles as follows: H(12)–O(22), 2.24 Å; N(12)–O(22), 3.02 Å; N(12)–H(12)–O(22), 140.0°. The final R index for (+)-83 was 0.0385.

Biological Methods. (a) *In Vitro* Enzyme Assay. Enzyme Preparation. Bovine lens AR was prepared using a modification of the procedure developed by Hayman and Kinoshita.[44] Bovine lenses were homogenized in three volumes of deionized H_2O at 0–4 °C with a tissue homogenizer set at a speed of 5–6 (Brinkman Instruments, Model PCV-110). The homogenate was centrifuged at 10000g for 15 min. Ammonium sulfate was added to the supernatant fraction to form a 40% saturated solution. This solution was stirred for 30 min, allowed to stand for 20 min, and then centrifuged at 10000g for 15 min. With this same procedure the recovered supernatant fraction was then sequentially fractionated with 50 and 75% saturated ammonium sulfate. The precipitate recovered from the 75% saturated ammonium sulfate solution was redissolved in 0.05 M NaCl and was dialyzed for 24 h in two changes of 10 L of 0.05 M NaCl. The dialyzed material was separated into 3.0-mL aliquots and stored at −20 °C.

Enzymatic Assay. Aldose reductase activity was determined spectrophotometrically by monitoring the oxidation of NADPH (340 nm, 37 °C) in a reaction mixture containing 30 mM sodium phosphate buffer, pH 6.2, 0.2 M $LiSO_4$, 1.2 mM NADPH, 5 mM glyceraldehyde, partially purified bovine lens aldose reductase, and vehicle or inhibitor. All of the inhibitors were dissolved in DMSO. The final concentration of DMSO in the reaction mixture was 1%. All of the assay components except glyceraldehyde were combined and incubated at 37 °C for 5 min prior to initiating the reaction with the addition of glyceraldehyde. The rate of oxidation of NADPH (decrease in optical density per minute) was calculated using the Beckman DU-7 kinetics software program (Beckman, Palo Alto, CA). To correct for the nonenzymatic oxidation of NADPH, the rate of NADPH oxidation in the presence of all of the reaction mixture components except glyceraldehyde was subtracted from each experimental rate. Under these conditions the rate of NADPH oxidation was linear with time and enzyme concentration. Each concentration of inhibitor was tested in duplicate, and IC_{50} values for several compounds were obtained from a linear regression analysis of the log concentration versus percent inhibition plots of the data.

(b) *In Vitro* and *ex Vivo* RBC Assay. *In vitro* experiments quantitating the effect of 41 on erythrocyte aldose reductase activity were performed with red blood cells collected from both rats and dogs. For the rat experiments, male Sprague–Dawley rats (Charles River) weighing between 150–170 g were randomized into groups of equal body weight, with six animals per group. After an 18-h fast, the animals were anesthetized with halothane, and 6 mL of blood was collected from the aortic arch into tubes containing EDTA (ethylenediaminetetraacetic acid, disodium salt). For the dog experiments, after an 18-h fast, 50 mL of blood was collected into tubes with EDTA, from the cephalic vein of each of three male beagle dogs weighing between 9 and 11 kg. Blood samples were centrifuged at 1000g for 10 min at 4 °C. The plasma and buffy coat were removed, and 1 mL of wet packed red blood cells from each rat was mixed with 2 mL of Hanks balanced salt solution (HBSS; Gibco, Gaithersburg, MD), enriched with 10 mM galactose with and without tolrestat or 41, at concentrations ranging between 1 and 5 × 10^{-8} M. The erythrocytes from the beagles were pooled prior to mixing with HBSS. The erythrocyte samples were kept in suspension and incubated for 3 h in an atmosphere of 95% air, 5% CO_2 in a Dubanoff metabolic chamber, oscillating at 60 cycles per min. In preliminary experiments, erythrocyte galactitol accumulation was proportional to the amount of galactose added to HBSS, for concentrations up to 15 mM, and to the length of the incubation for up to 5 h. Following the incubation, the erythrocyte suspensions were centrifuged at 1000g for 10 min at 4 °C. The supernatant fraction was then removed and the wet packed cells were frozen and stored at −20 °C prior to galacticol analysis.

For the *ex vivo* experiments, 5–10 mL of blood per animal was collected from groups of six rats or dogs, at selected times following their treatment with a single dose of vehicle, tolrestat 1.5 mg/kg for rats and 0.5 mg/kg for dogs, or 41, 0.2 mg/kg for rats and 0.025 mg/kg for dogs. Red blood cell samples from these animals were then individually processed and incubated as described above. There were no apparent differences between rats in the level of erythrocyte AR activity. However, these levels varied 2–3-fold between individual dogs. Due to this variability, dogs were randomized into groups with identical mean levels of erythrocyte AR activity for the *ex vivo* experiments.

Kinetic Studies. Kinetic studies in which the concentration of 41 and glyceraldehyde and/or NADPH cofactor were varied were performed under the conditions described above. For these experiments the concentration of glyceraldehyde ranged from 0.04 to 0.5 mM and the concentration of NADPH ranged from 0.05 to 1.2 mM.

(c) *In Vivo* Assay, Galactosemic Rats. Animals. Male Sprague–Dawley rats (Charles River, NY) weighing 70–90 g were randomized into groups of equal average body weight with six animals per group. The control group had free access to Purina

rat chow with 20% glucose. All of the other groups were fed chow containing 20% galactose (Bioserve, Springfield, NY) with or without the tested compound.

Test Procedures. On the fourth or fourteenth day of feeding, following a 3-h fast, animals were killed by decapitation. The lens and sciatic nerves were removed, weighed and rapidly frozen on porcelain plates cooled with dry ice. These samples were kept frozen at −20 °C prior to galactitol quantitation.

(d) *In Vivo* Assay, STZ Diabetic Rats. Animal Treatment. Male Sprague–Dawley rats (Charles River, NY) weighing 200–250 g were randomized into groups of equal average body weight with 12 animals per group. After an overnight fast, diabetes was induced in all of the experimental groups by an iv injection of streptozocin into the tail vein (Sigma Chemical Co.) at a dose of 60 mg/kg. For these injections streptozocin (STZ) was dissolved in cold (4 °C) 0.03 M citrate buffer, pH 4.5, and was used within 5 min of its preparation. Control animals were injected with vehicle alone. Plasma glucose concentrations were determined 2 days after the STZ administration and again on days 5 and 9. For all of these measurements blood was collected from the tail tip of each animal following a 4-h fast. Glucose was quantitated by the hexokinase method on an Abbott VP Analyzer. Animals were considered diabetic if the plasma glucose level exceeded 300 mg/dl. Animals with plasma glucose levels below 300 mg/dL were excluded from the study. Animals with plasma glucose levels above 550 mg/dL were removed from the study to reduce experimental variability. All of the animals had free access to water and normal rodent chow. The tested compound was suspended in 2% Tween 80 in saline and administered daily by gavage. Vehicle was administered to the control rats and to one group of diabetic animals which served as the diabetic controls. This dosing regimen was initiated on the day of STZ injection and continued thereafter, for 14 days. On the fifteenth day, following a 4-h fast, animals were anesthetized by halothane inhalation. A 5-mL blood sample was removed by cardiac puncture and transferred into tubes containing EDTA (Sherwood Medical, St. Louis, MO). Red blood cells (RBCs) were recovered from these samples following a 10-min centrifugation at 2000*g* and were immediately frozen. Animals were killed by cervical dislocation, and the lens and sciatic nerves were removed, weighed, and frozen on porcelain plates cooled on dry ice.

Analytical Procedures. Three methods were used to quantitate tissue polyol levels. The first and least sensitive was a modification of the method of Kraml and Cosyns[45b] which involved extraction of polyols with trichloroacetic acid, followed by periodate oxidation, and then a colorimetric analysis with chromotropic acid. This procedure is not very sensitive and cannot distinguish galactitol from sorbitol or *myo*-inositol. To confirm the results obtained with the periodate oxidation method, and to increase the assay specificity and sensitivity, tissue galactitol was also measured using a gas chromatographic procedure based upon a method previously described by Guerrant and Moss.[55] This procedure which involves conversion of aldoses to their corresponding aldonitrile acetates and polyol to their corresponding acetates, can distinguish the polyols, galactitol, sorbitol, and *myo*-inositol, and has a linear response for sorbitol and galactitol concentrations ranging between 0.5, the limit of detection, and 50 or 300 mg, respectively. While the gas chromatographic method for quantitating tissue levels of polyol is one of the most sensitive and specific assays, it requires extensive sample manipulation. To decrease the time required for sample analysis, a high-pressure liquid chromatographic procedure for quantitating tissue galactitol was recently introduced.[56] This procedure employs a pulsed amperometric detector linked to a Carbopac-PA anion-exchange column and a Carbopac-PA guard column fitted with an eluent degassing module (Done, CA). With this procedure, polyols, under slightly acidic conditions, weakly bind to an anion exchange column and are separately eluted with a 0–15 mM gradient of NaOH. This method has a limit of detection of 0.5 mg/mL of galactitol and a linear response for concentrations ranging between 0.5 and 300 mg/mL. The day to day coefficient of variation for concentrations ranging between 0.5 and 30 mg/mL was 3.6%. Over this same concentration range the recoveries of galactitol from the sciatic nerve and lens were 91.5 and 101.1%, respectively. Sample preparation for this method required galactitol extraction from tissue by homogenization in 0.3 N $ZnSO_4$, followed by neutralization with $Ba(OH)_2$ and centrifugation at 1000*g* for 15 min at 4 °C. Following the addition of preseitol, the internal standard, the supernatant fraction was immediately analyzed for galactitol. With all of the quantitation methods, polyol, sorbitol, and galactitol were expressed as nanomoles per milligram wet weight of tissue.

Statistical Analysis. Tissue polyol or galactitol levels in each drug-treated group were compared with those in the normal control and galactose-fed control groups by ANOVA and Dunnett's multiple comparison test. ED_{50} values were calculated with a nonlinear regression of the log of the dose versus tissue polyol or galactitol levels using the Wyeth-Ayerst HT Basic statistical package. For these analyses the data were corrected by subtracting the average background polyol or galactitol content found in each tissue of the normal rats fed 20% glucose.

Acknowledgment. We gratefully acknowledge Dr. K. Sestanj for helpful discussions and suggestions; Mr. J. DelliSanti for his contribution in the preparation of some compounds; Mr. B. Hofmann and his staff for the analytical data; Dr. D. Van Engen of Princeton University for the X-ray studies; Mr. M. Basso, Ms. M. Bock, Ms. R. Guilloud, and Ms K. D. Lai for assisting with the *in vitro* and *in vivo* studies; and Mrs. C. Delfino for typing the manuscript.

Supplementary Material Available: Crystal parameters and structure diagrams of **82** and **83**, atomic coordinates and anisotropic thermal properties, bond lengths and angles, and H atom coordinates for target spirosuccinimides (18 pages). Ordering information is given on any current masthead page.

References

(1) Pirart, J. Diabetes mellitus and its degenerative complications: A prospective study of 4,400 patients observed between 1947 and 1973. *Diabetes Care* **1978**, *1*, 168–188.
(2) Zimmerman, B. R. Influence of the degree of control of diabetes on the prevention, postponement and amelioration of late complications. *Drugs* **1989**, *38*, 941–956.
(3) Ziegler, D.; Mayer, P.; Muhlen, H.; Gries, F. A. The natural history of somatosensory and autonomic nerve dysfunction in relation to glycaemic control during the first 5 years after diagnosis of Type I (insulin-dependent diabetes mellitus). *Diabetologia* **1991**, *34*, 822–829.
(4) (a) The Diabetes Control and Complications Trial Research Group. The effect of intensive treatment of diabetes on the development and progression of long-term complications in insulin-dependent diabetes mellitus. *N. Engl. J. Med.* **1993**, *329*, 977–986. (b) Reichard, P.; Nilsson, B. Y.; Rosenqvist, U. The effect of long-term intensified insulin treatment on the development of microvascular complications of diabetes mellitus. *N. Engl. J. Med.* **1993**, *329*, 304–309. (c) Wang, P. H.; Lau, J.; Chalmers, T. C. Meta-analysis of effects of intensive blood-glucose control on late complications of type I diabetes. *Lancet* **1993**, 1306–1309.
(5) Krans, H. N. J. Insulin, glucagon, and oral hypoglycemic drugs. In *Meyler's Side Effects of Drug*, 11th ed.; NMG Dukes; Elsevier: Amsterdam, 1992; pp 889–902.
(6) The DCCT Research Group. Epidemiology of severe hypoglycemia in the Diabetes control and Complications Trial. *Am. J. Med.* **1991**, *90*, 459.
(7) Dvornik, D. *Aldose Reductase Inhibition: An approach to the prevention of diabetic complications;* McGraw Hill: New York, 1987; p 368.
(8) Masson, E. A.; Boulton, A. J. M. Aldose reductase inhibitors in the treatment of diabetic neuropathy. A review of the rationale and clinical evidence. *Drugs* **1990**, *39*, 190–202.
(9) Notvest, R. R.; Inserra, J. J. Tolrestat, an aldose reductase inhibitor, prevents nerve dysfunction in conscious rats. *Diabetes* **1987**, *36*, 500–504.
(10) McCaleb, M. L.; Sredy, J.; Millen, J.; Ackerman, D. M.; Dvornik, D. Prevention of urinary albumin excretion in 6 month streptozocin-diabetic rats with the aldose reductase inhibitor tolrestat. *J. Diab. Compl.* **1988**, *2*, 16–18.
(11) Robison, W. G., Jr.; Nagata, M.; Laver, N.; Hohman, T. C.; Kinoshita, H. H. Diabetic-like retinopathy in rats prevented with an aldose reductase inhibitor. *Invest. Ophthalmol. Vis. Sci.* **1989**, *30*, 2285–2292.
(12) Sima, A. A. F.; Prashar, A.; Zang, W. X.; Chakrabarti, S.; Greene, D. A. The preventive effect of long-term aldose reductase inhibition (Ponalrestat) on nerve conduction and sural nerve structure in the spontaneously diabetic BB-rat. *J. Clin. Invest.* **1990**, *85*, 1410–1420.

(13) Sima, A. A. F.; Greene, D. A.; Brown, M. B.; Hohman, T. C.; Hicks, D.; Graepel, G. J.; Bochenek, W. J.; Beg, M.; Gonen, B. The tolrestat study group. Effect of hyperglycemia and the aldose reductase inhibitor tolrestat on sural nerve biochemistry and morphometry in advanced diabetic peripheral polyneuropathy. *J. Diab. Compl.* **1993**, *7*, 157–169.
(14) Santiago, J. V.; Sonksen, P. H.; Boulton, A. J. M.; MaCleod, A.; Beg, M.; Bochenek, W.; Graepel, G. J.; Gonen, B. The tolrestat study group. Withdrawl of the aldose reductase inhibitor tolrestat in patients with diabetic neuropathy: effect on neural function. *J. Diab. Compl.* **1993**, *7*, 170–178.
(15) Sima, A. A. F.; Bril, V.; Nathaniel, T. A.; McEwen, J.; Brown, M. B.; Lattimet, S. A.; Green, D. A. Regeneration and repair of myelinated fibers in sural-nerve biopsy specimens from patients with diabetic neuropathy treated with sorbinil. *N. Engl. J. Med.* **1988**, *319*, 548–555.
(16) Boulton, A. J. M.; Levin, S.; Comstock, J. A multicenter trial of the aldose-reductase inhibitor, tolrestat, in patients with symptomatic diabetic neuropathy. *Diabetologia* **1990**, *33*, 431–437.
(17) Macleod, A. F.; Boulton, A. J. M.; Owens, D. R.; VanRooy, P.; Van Gerven, J. M. A. The North European Tolrestat Study Group. A multicentre trial of the aldose reductase inhibitor tolrestat in patients with symptomatic diabetic peripheral neuropathy. *Diab. Metab.* **1992**, *18*, 14–20.
(18) Publiese, G.; Tilton, R. G.; Williamson, J. R. Glucose-induced metabolic imbalances in the pathogenesis of diabetic vascular disease. *Diab. Metab. Rev.* **1992**, *7*, 35–59.
(19) Tilton, R. G.; Chang. K.; Puglisse, G.; Eades, D. M.; Province, M. A.; Sherman, W. R.; Kilo, W. R.; Williamson, J. R. Prevention of hemodynamic changes and increased vascular albumin filtration in diabetic rats by aldose reductase inhibitors. *Diabetes* **1989**, *37*, 1258–1270.
(20) Krans, H. M. J. Recent clinical experience with aldose reductase inhibitors. *J. Diab. Compl.* **1992**, *6*, 15–20.
(21) Hotta, N.; Sakamoto, N. Aldose reductase inhibitors. In *The Diabetes Annual/5*; Alberti, K. G. M. M., Krall, L. P., Eds.; Elsevier, Amsterdam, 1990; pp 330–361.
(22) Kirchain, W. R.; Rendell, M. S. Aldose reductase inhibitors. *Pharmacotherapy* **1990**, *10*, 326–336.
(23) Larson, E. R.; Lipinski, C. A.; Sarges, R. Medicinal chemistry of aldose reductase inhibitors. *Med. Res. Rev.* **1988**, *8*, 159–186.
(24) Sarges, R.; Schnur, R. C.; Belletire, J. L.; Peterson, M. J. Spiro hydantoin aldose reductase inhibitors. *J. Med. Chem.* **1988**, *31*, 230–243.
(25) Brazzell, R. K.; Mayer, P. R.; Dobbs, R.; McNamara, P. J.; Teng, R.; Slattery, J. T. Dose-dependent pharmacokinetics of the aldose reductase inhibitor imirestat in man. *Pharm. Res.* **1991**, *1*, 112–118.
(26) Dietrich, E.; Stracke, H.; Federlin, K. The effets of the aldose reductase inhibitor Statil on diabetic peripheral neuropathy. *Diabetologia* **1990**, *33* (Suppl.), A-167.
(27) Florkowski, C. W.; Rowe, B. R.; Nightingale, S.; Harvey, T. C.; Barnett, A. H. Clinial and neurophysiologial studies of aldose reductase inhibitor ponalrestat in chronic symptomatic diabetic peripheral neuropathy. *Diabetes* **1991**, *40*, 129–133.
(28) Greene, D. A.; Sima, A. A. F. Effect of aldose reductase inhibitors on the progression of nerve damage. *Diab. Med.* **1993**, *10* (suppl. 2), 315–325.
(29) Hotta, N.; Kakuta, H.; Ando, F.; Sakamoto, N. Current progress in clinical trials of aldose reductase inhibitors in Japan. *Exp. Eye Res.* **1990**, *50*, 625–628.
(30) Jaspan, J.; Maselli, R.; Herold, K.; Bartkus, C. Treatment of severely painful diabetic neuropathy with an aldose reductase inhibitor: relief of pain and improved somatic and autonomic nerve function. *Lancet* **1983**, No. 2, 758–762.
(31) Krentz, A. J.; Honigsberger, L.; Ellis, S. H.; Hardman, N.; Nattrass, N. A 12-month randomized controlled study of the aldose reductase inhibitor ponalrestat in patients with chronic symptomatic diabetic neuropathy. *Diab. Med.* **1992**, *9*, 463–468.
(32) Pitts, N. E.; Vreeland, F.; Shaw, G. L.; Peterson. M. J.; Mehta, D. J.; Collie, J.; Gundersen, K. Clinical experience with sorbinil - an aldose reductase inhibitor. *Metabolism* **1986**, *35* (Suppl. 1), 96–100.
(33) Stribling, D. Clinical trials with aldose reductase inhibitors. *Exp. Eye Res.* **1990**, *50*, 621–624.
(34) Sundkvist, G.; Armstrong, F. M.; Bradburg, J. E.; Chaplin, C.; Ellis, S. H.; Owens, D. R.; Rosen, I.; Sonksen, R. United Kingdom/Scandinavian Ponalrestral Trial. Peripheral and autonomic nerve function in 259 diabetic patients with peripheral neuropathy treated with ponalrestat (an aldose reductase inhibitor) or placebo for 18 months. *J. Diab. Compl.* **1992**, *6*, 123–130.
(35) Young, R. J.; Ewing, D. J.; Clarke, B. F. A controlled trial of sorbinil, an aldose reductase inhibitor, in chronic painful diabetic neuropathy. *Diabetes* **1983**, *32*, 938–942.
(36) Ziegler, D.; Mayer, P.; Rathmann, W.; Gries, F. A. One-year treatment with the aldose-reductase inhibitor ponalrestat, in diabetic neuropathy. *Diabetes Res. Clin. Pract.* **1991**, *14*, 63–74.
(37) Gill, J. S.; Williams, G.; Ghatei, M. A.; Hetreed, A. H.; Mather, H. M.; Bloom, S. R. Effects of the aldose reductase inhibitor, ponalrestat, on diabetic neuropathy. *Diabete Metab.* **1990**, *16*, 296–302.
(38) Giugliano, D.; Marfella, R.; Quatraro, A.; DeRosa, N.; Salvatore, T.; Cozzolino, D.; Ceriello, A.; Torella, A. Tolrestat for mild diabetic neuropathy: A 52-week randomized, placebo-controlled trial. *Ann. Intern. Med.* **1993**, *118*, 7–11.
(39) Spielberg, S. P.; Shear, N. H.; Cannon, M.; Hutson, N.; Gunderson, K. *In vitro* assessment of a hypersensitivity syndrome associated with sorbinil. *Ann. Intern. Med.* **1991**, *114*, 720–724.
(40) Humber, L. G. The Medicinal Chemistry of Aldose Reductase Inhibitors. In *Progress in Medicinal Chemistry*; Ellis, G. P., West, G. B., Eds.; Elsevier Science Publishers: New York, 1987, Vol. 24, pp 299–343.
(41) Sarges, R. Aldose Reductase Inhibitors: Structure-Activity Relationships and Therapeutic Potential. *Advances in Drug Research*; Academic Press: San Diego, 1989; Vol. 18, pp 139–175.
(42) Mander, L. N.; Sethi, P. Regioselective synthesis of β-ketoesters from lithium enolates and methyl cyanoformate. *Tetrahedron Lett.* **1983**, *24*, 2425.
(43) McKillop, A.; Bruggin, K. A. A study of the copper-catalyzed direct arylation of β-dicarbonyl compounds with 2-bromobenzoic acid. *Tetrahedron* **1975**, *31*, 2607–2619.
(44) Hayman, S.; Kinoshita, J. H. Isolation and properties of lens aldose reductase. *J. Biol. Chem.* **1965**, *240*, 877.
(45) (a) Dvornik, D.; Simard-Duquesne, N.; Kraml, M.; Sestanj, K.; Gabbay, K. H.; Kinoshita, J. H.; Varma, S. D.; Merola, L. O. Polyol accumulation in galactosemic and diabetic rats: Control by an aldose reductase inhibitor. *Science* **1973**, *182*, 1146. (b) Kraml, M.; Cosyns, L. A semi-automated determination of serum triglycerides. *Clin. Biochim.* **1969**, *2*, 373.
(46) (a) Brittain, D. R.; In *Third SCI-RSG Med Chem Symposium*; Special Publication No. 55, Lambert, R. W., Ed.; Royal Society of Chemistry, London, 1985; pp 210–240. (b) Stribling, D.; Brittan, D. R. Structure Activity Relationships of Aldose Reductase Inhibitors and Their Possible Use in Diabetic Complications. In *Innovative Approaches in Drug Research*; Harns, A. F., Ed.; Elsevier Science Publishers B. V.: Amsterdam, 1986; pp 297–313.
(47) Mylari, B. L.; Larson, E. R.; Beyer, T. A.; Zembrowski, W. J.; Aldinger, C. E.; Dee, M. F.; Siegel, T. W.; Singleton, D. H. Novel, potent aldose reductase inhibitors: 3,4-Dihydroxy-4-oxo-3-[[5-(trifluoromethyl)-2-benzothiazolyl]methyl]-1-phthalazineacetic acid (zopolrestat) and Congeners. *J. Med. Chem.* **1991**, *34*, 108–122.
(48) Sato, S.; Kador, P. F. NADPH-dependent reduction of the dog lens. *Exp. Eye Res.* **1990**, *50*, 629–634.
(49) Simard-Duquesne, N.; Greselin, E.; Dubuc, J.; Dvornik, D. The effects of a new aldose reductase inhibitor (tolrestat) in galactosemic and diabetic rats. *Metabolism* **1985**, *34*, 885–892.
(50) Dvornik, D.; Millen, J.; Hicks, D.; Cayen, M.; Sredy, J. The Pharmacokinetics of aldose reductase inhibitors. *Polyol Pathway And Its Role In Diabetic Complications*; Elsevier Science Publishers B. V.: Amsterdam, 1988; pp 61–71.
(51) Cayen, M. N.; Hicks, D. R.; Ferdinandi, E. S.; Kraml, M.; Greselin, E.; Dvornik, D. Metabolic desposition and pharmacokinetics of aldose reductase inhibitor tolrestat in rats, dogs and monkeys. *Drug Metab. Dispos.* **1985**, *13*, 412–419.
(52) Still, W. C.; Kahn, M.; Mitra, A. Rapid Chromatographic Technique for Preparative Separations with Moderate Resolution. *J. Org. Chem.* **1978**, *43*, 2923.
(53) Rogers, D. *Acta Crystallogr.* **1981**, *A37*, 734.
(54) Cromer, D. T.; Waber, J. T. *International Tables for X-Ray Crystallography*; Kynoch Press: Birmingham, England, 1974; Vol. IV, p 99.
(55) Guerrant, G. O.; Moss, C. W. Determination of monosaccharides as aldonitrile O-methyloxime, alditol and cyclitol acetate derivatives by gas chromatography. *Anal. Chem.* **1984**, *56*, 633.
(56) Dickerson, F. E., Jr.; Lou, M. F. Macro-quantitation of lens myo-inositol by anion exchange chromatography. *Curr. Eye Res.* **1990**, *9*, 201.